SPACE TELESCOPE SCIENCE INSTITUTE
Operated for NASA by AURA

Instrument Science Report WFC3 2008-01

WFC3 TV2 Testing: Calibration Subsystem Performance

S.Baggett
January 11, 2008

ABSTRACT

This report summarizes the behavior of the WFC3 calsystem, based upon data acquired during thermal-vacuum level tests performed in 2007 with the UVIS-2 (flight spare) and IR-1 (FPA129, pre-flight) detectors. The illumination patterns and features observed in the tungsten and deuterium flatfields are described and their characteristics evaluated in light of the calsystem requirements. Although two of the four tungsten bulbs burned out and a third was degrading by the end of TV2, the one good tungsten bulb and the UV deuterium lamp delivered, with a very small number of exceptions, illumination satisfying the flux requirement (>16.7 /s/pix) and the uniformity specification (< factor of two over the full field of view). The long-term stability needs (better than 5%) are met in many instances but not all. In addition, there are low-level (few percent) features in the flatfields which are seen to vary over time. Also noted was a tendency for UVIS and IR tungsten flatfields taken with MEB2 (instrument side 2) to be fainter by a few percent than those taken with MEB1. Finally, the analysis of the IR flatfields revealed that the early reads in a subarray ramp are distinctly non-linear when compared to later reads in the ramp; the OPUS calibration pipeline calwf3 and/or WFC3 FSW will need to be adjusted to handle these cases.

Introduction

The calibration subsystem (calsystem) is an internal stimulus for WFC3, designed to provide uniform illumination across the entire field of view for both channels. The resulting flatfields are intended for use in monitoring the health and status of various instrument

parameters such as gain, shutter travel and changes in flatfields as well as correcting ground flatfields for use on-orbit. A deuterium lamp (D2; no backup) provides the necessary UV flux for the UVIS channel, while tungsten bulbs provide visible and IR flux for both channels. There are four tungsten bulbs, nominally two per channel (a primary and a backup for each) though any lamp can be configured to be used with either channel.

For the UVIS channel, light from the D2 lamp or the tungsten lamp assembly is relayed to the detector through a hole located in the center of the UVM2 mirror (the hole is located at the pupil image of the OTA central obscuration). For the IR channel, light is directed from the tungsten lamp assembly to a reflective diffuser located on a paddle attached to the channel select mechanism (CSM). When the CSM is out of the beam path, the diffuser is in the IR beam path.

The calsystem is required to provide 1) illumination uniform to better than a factor of two over the field of view, 2) stability over hour (<1%/pixel) and year (<5%) timescales and repeatability (over a year) to +/- 50K color temperature, and 3) flux from 200-2000nm at the level of at least 10K e^- in 10 minutes (~16.7 e^-/s/pix) for all spectral elements. This report summarizes the characteristics of the calsystem data taken during 2007 thermal-vacuum instrument-level testing and compares the results to the specifications.

Observations and Analysis

The UVIS and IR calsystem exposures analyzed were drawn from four different TV programs, distinguished by the first four characters of the image filenames: iu23 (calsystem flatfield proposals), iu28 (science monitor), i61g (system functional), and i9v9 (system functional, aliveness test portion).

The UVIS flatfields were full-frame, unbinned, nominal gain setting (1.5 e^-/DN), default bias offset (setting 3, ~2500 DN), four-amp readouts although some single amp readouts were also included. The majority of CCD images were taken at -78C, somewhat warmer than the nominal -83C due to a lien against the UVIS-2 flight spare thermo-electric cooler. Each tungsten lamp was used with the UVIS channel in order to check the relative illumination levels of the lamps. The deuterium exposures were all taken at medium current to minimize aging of the lamp (high current has been shown to age the lamp faster than medium, ISR 2003-11). All images were processed through calwf3, performing the overscan correction (BLEVCORR) only and using versions of CCDTAB and OSCNTAB generated in Mar 2005 and Nov 2003, respectively.

The IR flatfield set consisted of full-frame and 64x64 subarray readouts; the IR detector was cooled to 147-150K (IRFPATMP header keyword). Images were processed through calwf3, performing only the data quality initialization, multiaccum zero read subtraction, and bias level substraction (as computed from reference pixel level); no dark correction was performed (effect from overall dark current level, is not significant, amounting to <0.5% of the signal in the two narrowest filters and <<0.1% in most other filters; effects from bad pixels are minimized by using clipped median statistics).

UVIS Tungsten Exposures

Image Features

Two typical UVIS calsystem flatfields are shown in Figure 1. For completeness, thumbnails of TV2 tungsten flatfield for each filter are shown in Appendix B (optimum viewing is on-screen, not paper). The notable features are described in detail below.

Figure 1: Full-frame, four-amp readout tungsten calsystem flatfields in F390W, shown with the same stretch (+/-30%) with an inverted greyscale. At left is the most recent image, at right is an image taken in 2005, before the glint issue was identified and addressed. Quadrants in this figure, and all subsequent figures, are shown in the nominal position (labelled A,B,C,D).

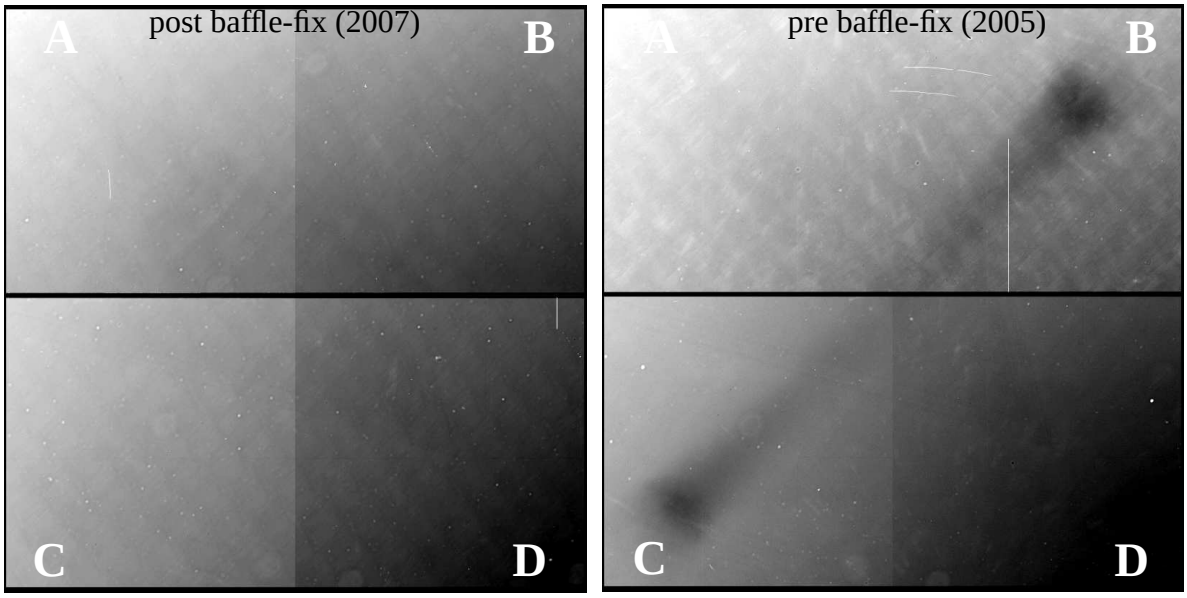

- As discussed in the report on the ambient test calsystem flatfields taken with UVIS-2 in April 2007 (ISR 2007-14), the prominent glints in amps B and C are gone, thanks to painting of the baffle tube between the filter wheel assembly and the shutter.

- There is an overall gradient across the field of view, from a low near the outer corner of quadrant A to a high near the outer corner of quadrant D (~30% across entire FOV). This is an artifact of the optical design of the UVIS channel: the detector is tilted such that the amp A corner is further from, and amp D is closer to, the hole in the M2 mirror through which the calsystem beam passes (G.Hartig, priv.comm.).
- The flare in quadrant A, extending into a faint diamond shape which spans the field of view from the A quadrant to the D quadrant (e.g., see F200LP image in Appendix B), is present as it was in previous UVIS-1 test data (ISRs 2007-14, 2005-09). Detailed investigation and troubleshooting during TV2 revealed that this feature is caused by glints within the UVIS detector housing (ISR 2007-21); the area causing the glints has been masked in the UVIS-1 (flight) detector to prevent the reflections.
- The outer corners of each quadrant show small arc-shaped glints at the level of a couple percent (a pair in quad C; e.g., see F200LP image in Appendix B). These were present in earlier ambient data taken with UVIS-2 as well as in earlier data taken with UVIS-1. They are not visible in external flatfields though similar arc features have been seen in images containing (heavily exposed) point sources.
- In the upper right of quadrant B is a small ‘shadow’ feature. Narrowband flatfields show closely-spaced fringes in this area, a signature of rapidly-changing thickness (and therefore sensitivity) of the CCD detection layer.
- Extended donut-like artifacts (about 150-250 pixels in diameter) can be seen in some flatfields, due to particles on the filter. Smaller spots (~10-40 pixels in diameter) are due to dust on the CCD windows.
- UV flatfields, both tungsten and deuterium, show the normal crosshatch pattern which is a result of the detector structure.
- As expected, narrowband images (particularly at redder wavelengths) show fringing due to interference within the detector layers (see images in Appendix B).
- As can be seen from the images in Appendix B, a small number of flatfields show anomalous features attributed to artifacts on the filter (e.g., scratches). These include FQ387N, with a diffuse horizontal band of light (the stronger, more diagonal features are thought to be glint from the housing, fixed in the flight detector), F410M, with scattering from beveled filter edges, F657N and F658N (horizontal and vertical bands of scattered light which can be 10’s of percent higher than surrounding level), and some faint scattered light in FQ508N/FQ575N and FQ619N/FQ750N. Note: these features are accentuated by the unusual calsystem beam; flatfields with HST-like illumination (from ground stimulus CASTLE) do not show these features.

Overall, the tungsten flatfields meet the uniformity specification, with the exception of F410M, F657N, and F658N, where flux levels in small regions of the flatfields can exceed a factor of two over the overall level. In these cases, the failure to meet the requirement is due to the filter, not the calsystem.

Image Flux Levels

As mentioned in the Abstract, two of the tungsten bulbs, #2 and #4, showed dramatically declining countrates along with declining current levels at lamp turn-on. These two lamps eventually burned out after a month of relatively low usage; plots of the flux decline are included in the IR Tungsten Exposure section. A third bulb, #3, was exhibiting some flux decline by the end of TV2 testing as well; inspection after TV2 showed the characteristic bluish tungsten haze on the interior of the glass envelope normally indicative of a failed bulb. This type of tungsten bulb (incandescent lamp filled with krypton, manufactured by Welch Allen) had survived rigorous lifetime tests. Expected lifetimes were on the order of 1500 hrs; only about 10% of that was achieved. Furthermore, the lamps in the instrument had survived complete burn-in and environmental tests by the GSFC Materials Branch. Investigation of the lamp failures is on-going but initial inspections revealed that the lamps had developed cracks due to mechanical stress; the cracks were not in the glass itself but rather in the epoxy holding the lamps and leads to their rings (C.Powers, priv.comm.). Once a crack develops, the gas within the glass envelope escapes, causing the filament to heat up, and burn out. New, more rugged tungsten bulbs (improved glass, thicker filaments, better lead design) were procured from Carley and the installation procedures were reviewed and revised to minimize any unnecessary stresses during the assembly build-up in order to ensure that future bulbs do not suffer premature burn-out. For the purposes of this report, the flux levels used to evaluate compliance with requirements has been restricted to results from measurements of the only apparently-stable lamp (#1).

Table 3 in Appendix A lists the UVIS-2 tungsten lamp #1 countrate results; tabulated are filter name, instrument side (MEB1 or MEB2), CCD temperature, number of images in that filter/MEB/temperature group, average countrates in chip 1 (quads A/B), in chip2 (quads C/D), and over the full field of view. Averages for full-filter flatfields were taken across each chip excluding a boundary of 10 pixels on all sides. Quad filter flatfields contain different bandpasses in each quadrant of the WFC3 field of view; statistics for these filters were obtained from the central 400x400 pixels within each quadrant. All countrates have been converted to e^- using gain = 1.5 e^-/DN.

Note that flatfields taken with different sides of the instrument were analyzed separately, to allow a check of whether the different electronics boxes produce different countrates. Not all filters were obtained with both sides of the instrument; from the small number that were, differences between MEB sides were usually 1-2% or less but could be higher (e.g., f555w, where MEB2 flats were ~5% fainter than those taken with MEB1). While some flatfields were taken at off-nominal temperatures (~ +22C and ~ -3C), only those taken at ~ -78 and ~-50 are presented here. Dark current has not been removed from the flatfields but its contribution is very low, ~0.5 e^-/hour/pix (Martel, 2007). The TV2 data show that flux levels in the visible filters meet the CEI specification of 16.7 e^-/s/pix. Some UV filters

(f336w, f343n, f390m, f395n, fq387n, fq422m, and fq436n) do not meet the requirement; however, higher countrates for five of the seven are available using the calsystem's deuterium lamp (see later section). A final note: spectral measurements of some of the new Carley bulbs in the lab have shown that they produce ~20% lower flux than the Welch Allen bulbs; if this should prove to be the case with the flight tungsten lamps, there will likely be one additional filter (F469N) which will have less flux than specified by the requirement.

Tungsten Lamp Repeatability

More than one flatfield was taken for a small number of filters with lamp #1. In these cases, the images were separated by more than a day, so only relatively long-term stability could be evaluated. Short-term behavior will need to be evaluated in the next TV. Despite being an apparently good lamp, lamp #1 repeatability did not meet the long-term stability requirement (better than 5% over 1 year): out of 13 configurations, 7 showed variations higher than 5%. For completeness, the specifics are tabulated in Table 1; note, however, that since the new replacement bulbs are from a different manufacturer, these results should not be taken as an indication of how the new bulbs will perform. The table lists the configuration, number of images in that configuration, the number of days spanned by the images, along with the average, minimum, maximum, and median countrates for the images. The last column shows the percent difference between the highest and lowest countrate image.

Table 1. UVIS tungsten lamp #1 countrate repeatability

configuration	num images	time span covered (days)	average e^-/s/pix	stddev e^-/s/pix	median e^-/s/pix	min e^-/s/pix	max e^-/s/pix	variation (percent)
F467M, MEB1	3	28	98.9	0.8	99.3	98.0	99.3	1.4
F502M, MEB1	3	30	56.3	2.7	57.5	53.2	58.2	8.9
F502N, MEB2	4	44	55.0	1.7	55.5	52.7	56.3	6.6
F555W, MEB1	6	82	2846.0	29.5	2858.1	2798.4	2871.1	2.6
F555W, MEB2	3	41	2709.3	199.6	2779.4	2484.1	2864.4	14.0
F625W, MEB1	6	101	6628.1	269.7	6729.4	6129.3	6864.0	11.1
F625W, MEB2	3	29	6473.3	346.7	6664.6	6073.2	6682.2	9.4
F645N, MEB1	6	101	404.9	11.2	401.7	391.8	420.5	7.1
F645N, MEB2	3	29	402.7	12.2	409.6	388.6	410.0	5.3
F657N, MEB1	4	101	680.0	21.1	682.6	654.7	700.3	6.7
F657N, MEB2	4	44	673.3	15.7	680.4	649.8	682.6	4.9
F814W, MEB1	7	82	19739.2	238.6	19820.1	19342.7	20020.6	3.4
F814W, MEB2	3	41	19657.0	352.9	19663.6	19300.8	20006.5	3.6

In addition, image ratios were generated from flatfields within a given configuration (same filter, instrument side, and temperature). As seen previously in ambient calsystem UVIS-2 flatfields (ISR 2007-14) and in a number of UVIS-1 images as well, the ratios show what appear to be a very low-level hysteresis effects. Typically most noticable in image ratios, the effect is also occasionally seen in single images, e.g., a 900 sec dark taken with UVIS-2 on Mar 25,2007. Examples of the types of patterns seen in the TV2 data are illustrated in Figure 2. At left is an F625W flatfield image ratio, containing low-level roughly diagonal streaks from B quad to C quad, attributed to shutter edge effects (exposure times were 0.5 sec) and a very faint 'bowtie' in each chip (slowly curving, horizontal shape), cause still unknown. At right is an F814W flatfield image ratio showing the field point pattern across the FOV (small, extended PSF-like spots in locations matching the images taken for alignment checks), the traditional 'bowtie' shape in C/D (though it's narrower than in the F625W ratio) and a new shape: large triangles at the sides of A/B. In addition, there are other very low level features visible, implying that there were slight changes in illumination and/or QE level between the two flats used to generate the ratio: the arclets in the outer corners of each quad, the small QE feature in the outer corner of quad B, the diagonal lines across the FOV as a whole, the large semi-circular lines in A/B, and finally, a slight suggestion of changes in the 'flare' feature.

Figure 2: Two full-frame calsystem flatfield ratios; display is a hard, inverted stretch of +/- 1% to highlight features (see text). At left is F625W ratio of images taken 14 days apart; at right is F814W ratio of images taken 5 days apart.

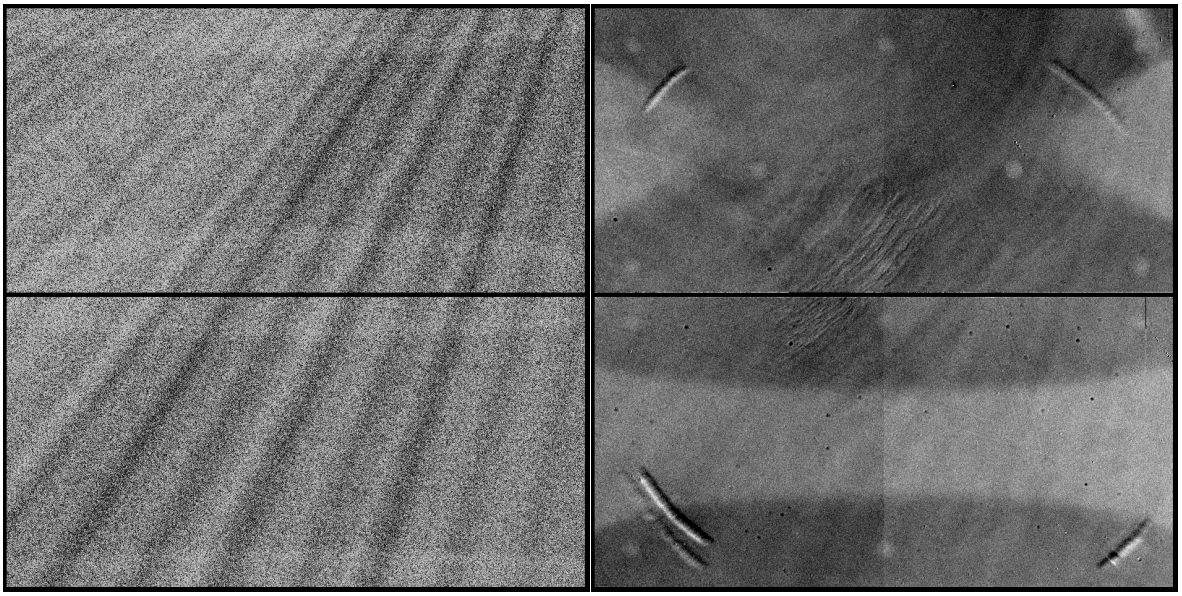

UVIS Deuterium Exposures

Image Features

As noted in the report on ambient calsystem flatfields (ISR 2007-14), the deuterium flatfields are now relatively flat in comparison to the images from the first ground testing which showed 5-10x gradients across the field of view from C quadrant up through B quadrant (ISR 2005-09). Figure 3 shows two deuterium flatfields from TV2, the left image taken with F218W and right with F390W, shown in an inverted stretch. The characteristic background cross-hatch pattern seen in all UV flatfields is present; the features are typically a few percent peak to peak but very repeatable from image to image (see next section). The overall gradient across the FOV is ~5-15% though the F390W shows more of a downturn, at the level of a few 10's of percent, in the outer corners of quadrants B and D. The small white spots are painted pinholes. Excluding the small spots and the extreme roll-offs at the edge which seem to be worse in redder filters, overall the deuterium flatfields meet the uniformity specification requiring the illumination pattern be flat to better than a factor of two across the field of view.

Figure 3: UVIS calsystem deuterium flatfields (F218W at left and F390W at right) shown in inverted stretch with scale at +/-20%.

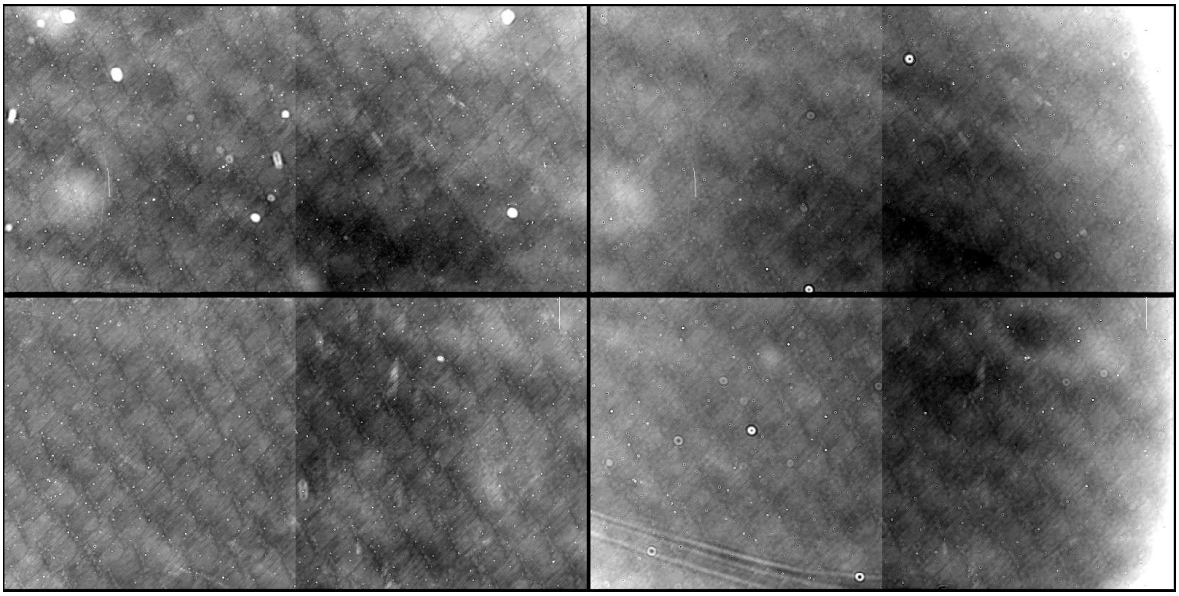

Image Flux Levels

The flux levels measured in the TV2 deuterium calsystem flatfields are provided in Table 4 in Appendix A. Listed are the filter name, instrument side, CCD temperature (from IUVDETMP keyword), observation date, exposure time of image, and median level as measured across entire field of view. Results for the four bandpasses of each quad filter are reported separately (filternames FQ*); statistics are based upon the central 400x400 pixel area in the appropriate quadrant. All exposure levels have been converted to e^-/s/pix using 1.5 e^-/DN. The flux requirement is met for all but the quad filters FQ436N and FQ437N; countrates are 15.7 and 12.5 e^-/s/pix respectively, or about 5% and 25% below the specification.

The specification could be met by operating the deuterium lamp at the high current setting (doubling the countrate); however, lamp lifetime test results showed that the medium current setting minimized degradation in lamp performance and provided the most stable short and longterm throughput (ISR 2003-11). Lamp operations are expected to be restricted to medium current only.

Deuterium Lamp Repeatability

Based upon overall count rates, the deuterium flatfields appear to be fairly repeatable (see ratio column in Table 4 in Appendix A). Images with a given filter are typically within 1-3% of each other, though there are occasional excursions of 5-10%. The largest number of images were taken with F218W; in this case, images taken with MEB1 generally had count rates ~5% higher than those taken with MEB2 (average of 897 versus 862 e^-/s/pix). In addition, it should be noted that there were occasional turn-on delays during TV2, when the D2 failed to fire during the nominal 2 seconds. The lamp eventually would fire, taking anywhere from a minute up to ~10 minutes; obviously any flatfield being taken during that time would have no D2 flux (and are not included in here) while subsequent flatfield exposure levels after the delayed turn-on exhibited the expected flux levels.

Image ratios of the deuterium flats showed that pixel-to-pixel, they were generally flat to 1% or better (all ratios in a given filter were formed using the earliest TV2 flatfield for that filter as a baseline). Some ratios showed evidence for new very small spots, attributed to dust on the channel select mechanism; in addition, there were occasional small differences in the normal flatfield characteristics such as the UV cross-hatch pattern (0.5% or less) or small scale mottling (e.g, in FQ437N quad; 0.5% or less), or e.g., in the illumination of dust and/or painted pinholes on the filter. However, flatfield ratios from one filter (F218W) showed more significant features, with strengths of up to ~2% peak-to-peak; furthermore, those ratio features varied with time. While other filters did not exhibit time-dependent behavior, this is likely due to the sparser sampling: only ~3 flats were taken in the majority of UV filters during TV2 as part of the calsystem checks; there were significantly more deuterium flats taken in F218W as it was part of the system functional and science monitor programs as well (results shown here are based on flats taken at -78 only).

Figure 4 shows image ratios for F218W (left) and F336W (right) with an inverted, hard stretch of +/-5% used to highlight the features. Particularly noticable in the F218W ratio, there are broad, diffuse "waves" spreading across the FOV, crossing the chip gap (implying the issue is not with the chips). While the source of the features is still unknown, it can not be on the filter as the identical pattern is seen, albeit very faintly, in other filters, e.g., F336W ratio. Tracing the level of one of the most prominent “waves” through each available F218W ratio image, the effect is seen to change with time, growing to ~2% peak to peak on days 193/198, nearly gone on day 204,and back up to ~2% on day 222 (see Figure 5). Cuts through image ratios from other filters were similar to (F225W, F275W), or flatter than (F200LP, F280N, F300X, F390W), the F336W results shown in Figure 5, with the most prominent feature at ~1% peak-to-peak.

Figure 4: Deuterium flatfield image ratios, F218W at left, F336W at right. Both are shown with a hard, inverted stretch of +/- 5%.

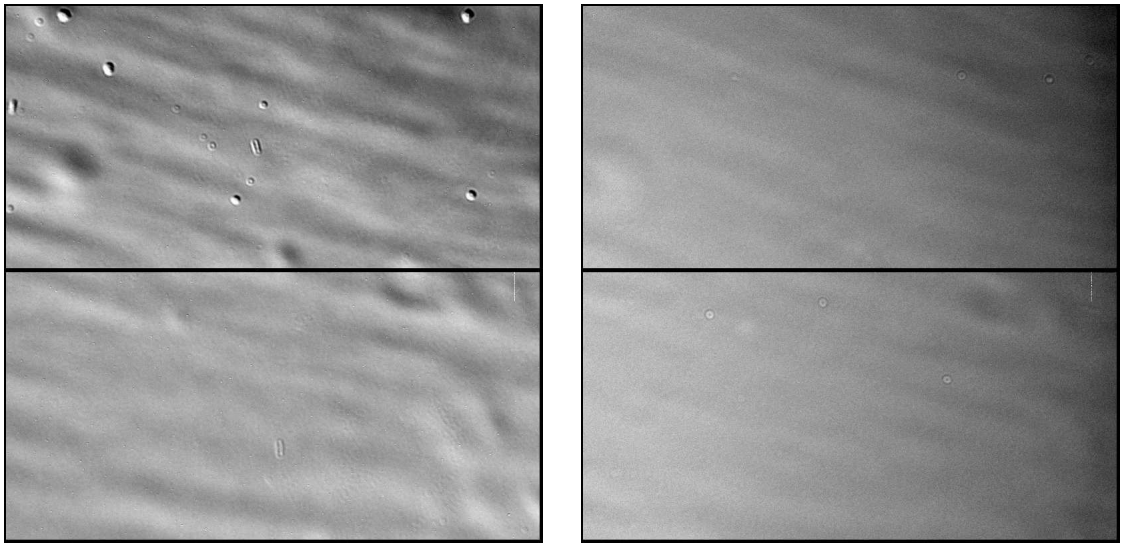

Figure 5: Cuts through deuterium flatfield image ratios using F218W (left) and F336W (right); each cut is an average of 150 columns through quadrant D.

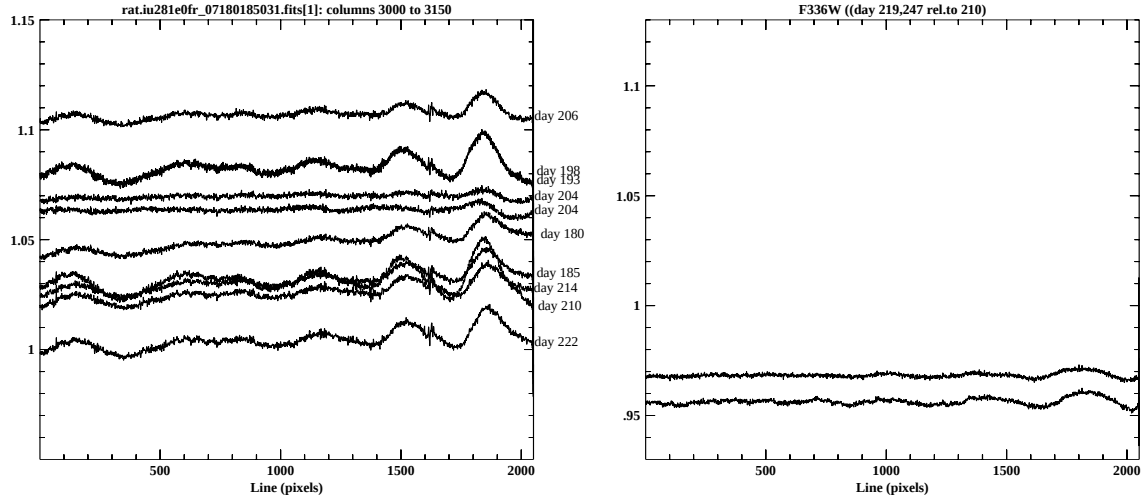

IR Tungsten Exposures

Image Features

Two typical IR calibration subsystem tungsten flatfields are shown in Figure 6, F105W at left and F167N at right, shown at +/-30% inverted stretch with contours overlayed at 0.5% intervals. Images in other IR filters are included in Appendix B. The illumination pattern generally meets the uniformity requirement (better than a factor of 2 across the FOV). As can be seen from the figure, with the exception of the cross-hatch, scratch-like features covering the FOV and the thicker, horizontal scratches near the right center edge (characteristic of this device, FPA129), the flatfields are fairly smooth. The illumination level

peaks in the upper right quadrant and drops as one moves towards the left edge of the FOV; at the edge, fluxes are down ~30-40% compared to the peak. In addition, there is a downturn in the lower right corner (~50x50 pixel region) where the flux drops to ~60% that of the peak and a similar, though smaller region in the upper right corner of the FOV (these may be the shadows of the screw heads on the diffuser paddle, H.Bushouse, priv.comm.). The pattern remains relatively similar across the IR filters, with small changes (~10%) visible in the reddest filters (F160W, F164N, F167N).

Figure 6: IR calsystem tungsten lamp flatfields, displayed with inverted greyscale stretch of +/-30%, with contours at 0.5% intervals.

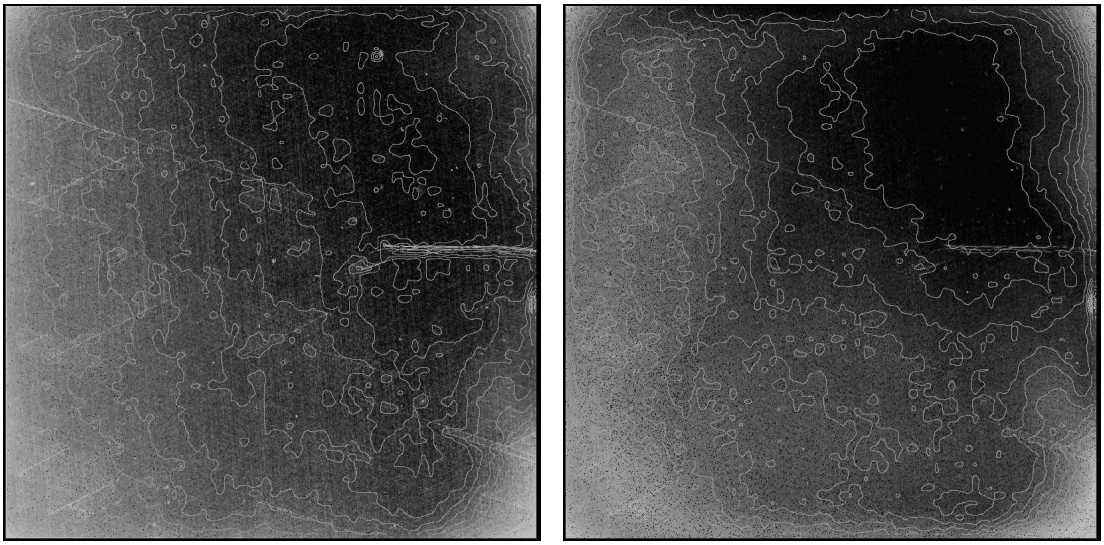

Flux Levels

As mentioned in the UVIS tungsten lamp section, two bulbs (#2,#4) burned out during TV2 and a third (#3) was starting to show some flux degradation by the end of the test. All bulbs are being replaced with an improved design from another vendor; however, for completeness, Figure 7 illustrates the observed flux decline in the two failed bulbs: with relatively light use, bulb #2 was dead within ~30 days. Bulb #4 showed some decline over the first 30 days as well; later, a UVIS flatfield with lamp #4 in early August showed that its output had dropped to 10% of the expected countrate and by the next observation in September, there was no more signal.

Figure 7: Tungsten lamp 2 and 4 flux decline as measured from IR calsystem flatfields.

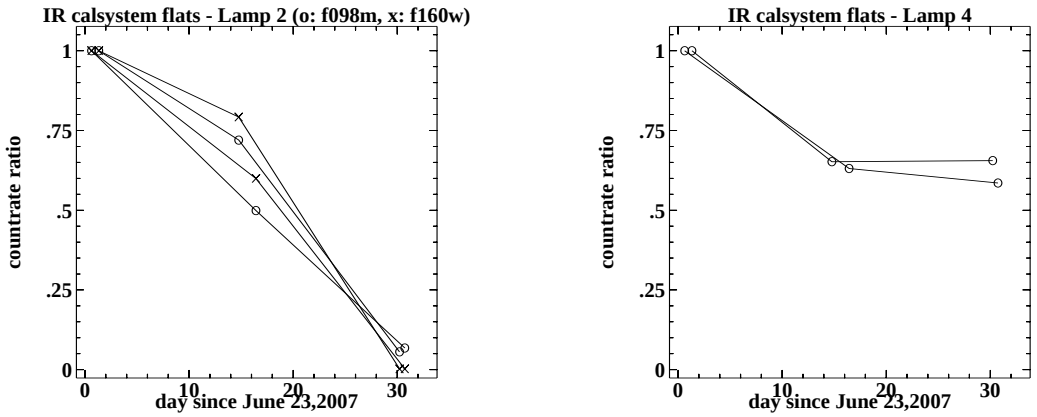

Table 5 in Appendix A lists the IR tungsten lamp countrate results; tabulated are filter name, lamp number, instrument side (MEB1 or MEB2), observation date and time, sample sequence type and number of reads, image size, median countrates over the full field of view, and ratio (countrate compared to the earliest TV2 flatfield countrate in that same filter). All countrates have been converted to e^- using gain = 2.0 e^- /DN. As can be seen from the median countrates, the tungsten lamp flux levels in all IR filters meet the requirement (16.7 e^- /s) though it should be noted that two of the narrowbands (F126N, F128N) are close enough to the spec that if the new tungsten bulbs come in ~20% fainter than the ones used in TV2, the flatfields in those filters will no longer meet the flux spec.

As for UVIS data, IR data from the two instrument sides were analyzed separately. Not all filters were obtained with both sides of the instrument but from the number that were, some configurations showed effectively no difference in median countrate on each instrument side (F098M+lamp1, F098M+lamp2, F167N+lamp1, F167N+lamp3), while other combinations (F125W+lamp 1, F160W+lamp1, F160W+lamp3) exhibited differences in median countrate of ~2-5%. These variations were in the sense as seen on the UVIS side: flats taken with MEB2 were slightly fainter than those taken with MEB1.

Tungsten Lamp Repeatability in IR

Due to schedule constraints during TV2, multiple flatfields were obtained for only a small number of IR filters. However, for those that were, the median countrates tabulated in Appendix A show that the tungsten lamp can be quite stable on short timescales: better than 1% in the relatively large F125W image sets (used for gain measurements). On longer timescales, the repeatability in most configurations is better than the 5% requirement. There are some apparent discrepancies although they are not due to the lamp. That is, in

F098M+lamp1+MEB1 (one image ~15% lower in flux than the rest) and F167N+lamp1+MEB1 (one image ~18% lower in flux than the rest), the out-of-family images are full-frame readouts while the rest of the set were subarrays. The issue has been traced to an apparent non-linearity in the subarray ramps, where the initial 1-2 reads in each ramp have significantly lower counts than expected based upon later reads in that ramp, resulting in an artificially higher final countrate. As can be seen in the tabulated ratios for the subarray data, however, the subarray countrates are quite repeatable (i.e., the low initial reads are repeatably low). The FSW and calwf3 pipeline process will be evaluated for possible improvements; meanwhile, a manual workaround has been developed but given that the subarray data is so repeatable and that the data presented here are not the final flight lamps, the subarray flatfields here have not been reprocessed to fix the issue. *Observers in need of absolute countrates from Appendix A should use the full-frame results only.* The remaining outliers, the F098M+lamp3 flatfields with flux 7-9% lower than at the beginning of TV2, are attributed to lamp degradation; as mentioned in the UVIS section, examination of bulb #3 after TV2 showed that it had developed a crack in its envelope and showed the characteristic bluish tinge of tungsten on the glass.

Finally, image ratios of the tungsten IR flats show that while they were generally flat, there are small spots and regions that vary with time (also noted by T.Brown, priv.comm.). Two examples are shown in Figure 8: an F125W image ratio (images taken 3 days apart) and an F160W image ratio (images taken 8 days apart). Clearly visible are changes in the left and lower edges of the images as well as a small number of spots. Table 2 presents median countrates in a small number of areas (the two edges and two of the spots) as a function of time; variations range from 0.5% up to ~10%. The cause of these features, suspected to be on the detector window, is not currently known.

Figure 8: IR tungsten flatfield ratios shown in inverted +/-5% inverted greyscale; F125W is at left, F160W is at right.

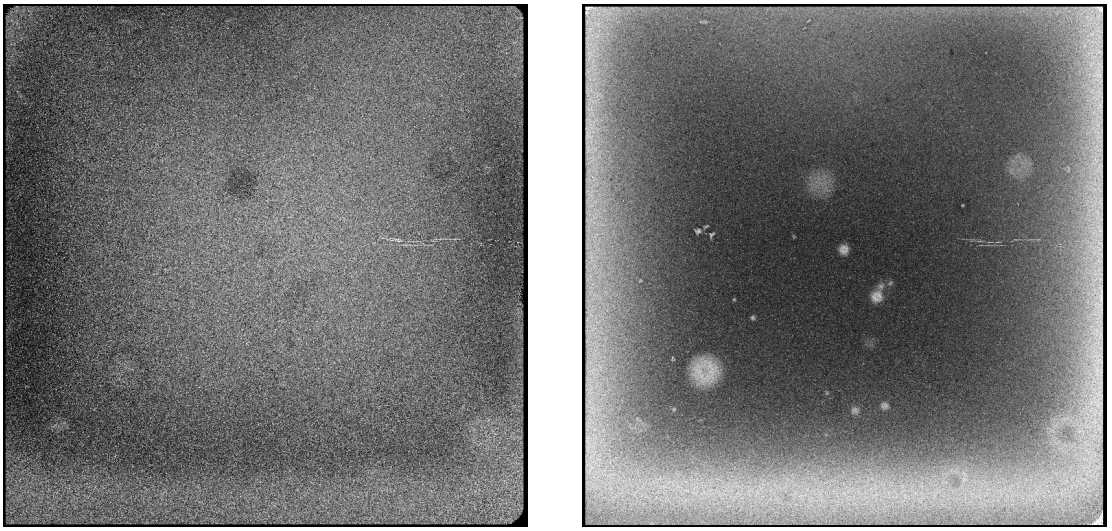

Table 2. Countrates within selected regions of F160W IR tungsten lamp #1 flatfields.

instrument side	date-obs	sampseq (nramp)	sqsize	lower edge		left edge		spot1		spot2	
				e-/s/p	ratio	e-/s/p	ratio	e-/s/p	ratio	e-/s/p	ratio
meb1	07-12-2007	step25 (8)	1024	363.6	1.000	337.1	1.000	455.2	1.000	372.6	1.000
meb1	07-17-2007	step25 (8)	1024	359.6	0.989	335.7	0.996	462.5	1.016	370.2	0.993
meb1	07-25-2007	step25 (8)	1024	364.6	1.003	354.5	1.051	472.5	1.038	375.3	1.007
meb1	07-30-2007	spars10 (15)	1024	359.7	0.989	331.8	0.984	452.0	0.993	368.3	0.988
meb1	08-02-2007	step25 (8)	1024	362.4	0.997	336.5	0.998	461.5	1.014	372.3	0.999
meb1	10-02-2007	step25 (8)	1024	364.6	1.003	340.7	1.011	462.2	1.015	373.0	1.001
meb2	06-26-2007	rapid (6)	1024	330.2	1.000	307.5	1.000	431.1	1.000	339.5	1.000
meb2	06-29-2007	rapid (7)	1024	366.6	1.110	342.5	1.114	463.1	1.074	376.2	1.108
meb2	07-05-2007	step25 (8)	1024	365.1	1.106	340.9	1.109	458.8	1.064	374.4	1.103
meb2	08-09-2007	step25 (8)	1024	366.3	1.109	336.1	1.093	432.9	1.004	371.6	1.095

Conclusions

The WFC3 calsystem flatfields from TV2, obtained with the UVIS-2 (spare) and IR-1 (FPA129 pre-flight) detectors, have been analyzed. Details of the illumination patterns were discussed, countrates tabulated, and image repeatability investigated. The results have been evaluated in light of the uniformity, flux, and long-term stability specifications.

The UVIS tungsten flatfields (with bulb #1) meet the uniformity requirement overall though there are three filters (F410M, F657N, F658N) which show small regions that fail the spec. The flux level requirement is met for all but seven filters, of which five can be obtained with the deuterium lamp with countrates which do meet the flux spec. The long-term stability requirement (better than 5%) was not met: some filters showed variations of 10-15% over a time-span of 10's of days. Some very low-level features (~1%) possibly a hysteresis effect, are noticable in image ratios.

The UVIS deuterium flatfields meet the uniformity requirement and are generally flat to ~10% though the illumination in the outermost corners of quad B/D drops off in a few filters by 10-30%. All but two UV filters meet the flux specification at medium current; at high current, the countrate in these filters (FQ436N, FQ437N) would easily meet the spec but to conserve lamp lifetime, operations are expected to be restricted to medium current. The flatfields are generally repeatable to within a few percent though there are occasional

deviations of 5-10%. Some lower-level features (at worst, ~2% peak to peak) were found to vary over the course of TV2. Finally, the lamp sometimes required minutes to turn on; to date, it always eventually came on; operational use of the lamp will take this into account (e.g., building in sufficient numbers of D2 flats that losing the occasional flat is not a problem).

The IR tungsten lamp #1 flatfields typically meet the uniformity specification and flatfields in all filters currently meet the flux requirement (if the new tungsten bulbs are ~20% fainter than those used in TV2, there will be ~two filters that will fail the flux spec). The flatfield repeatability was generally very good in the IR with lamp #1; outliers were traced to processing glitch. Image ratios did show some low-level features which changed over time; the cause for these is currently unclear. Flatfields in TV3 will need to be carefully monitored for these effects.

Acknowledgements

Thanks are due to the WFC3 team members who supported the thermal vacuum tests.

References

Baggett, S., “WFC3 Ambient-2 Testing: Calibration Subsystem Performance,” WFC3 Instrument Science Report WFC3-2007-14, May 2007.

Baggett, S., “WFC3 Thermal Vacuum and Ambient Testing: Calibration Subsystem Performance,” WFC3 Instrument Science Report WFC3-2005-09, March 2005.

Baggett, S., and Quijada, M., “Lifetime Test of a Deuterium Lamp for the WFC3 Calibration Subsystem,” WFC3 Instrument Science Report WFC3-2003-11, Nov 2003.

Brown, T., “WFC3 TV2 Testing: UVIS Channel Glint,” WFC3-2007-21, Oct 2007.

Martel, A.R., “WFC3 TV2 Testing: UVIS-2 Dark Frames and Rates,” WFC3-2007-26, Nov 2007.

Appendix A. Calsystem Countrates

Table 3. UVIS tungsten lamp #1 flatfield countrates from TV2.

filter	instrument side	CCD temp	num images	chip 1 e^-/s/pix	chip 2 e^-/s/pix	average e^-/s/pix
f200lp	MEB1	-78.1	1	27258.8	28650.9	27954.8
f336w	MEB1	-78.1	1	3.2	3.3	3.2
f343n	MEB2	-78.1	1	1.9	1.9	1.9
f350lp	MEB1	-78.3	1	29399.1	31054.6	30226.9
f390m	MEB2	-78.5	1	10.8	11.4	11.1
f390w	MEB1	-78.5	1	80.4	85.1	82.8
f395n	MEB2	-78.3	1	5.4	5.6	5.5
f410m	MEB1	-77.9	1	27.6	30.8	29.2
f410m	MEB2	-78.1	1	26.5	30.8	28.7
f438w	MEB1	-78.1	1	134.6	143.4	139.0
f467m	MEB1	-78.4	3	94.5	103.2	98.9
f467m	MEB2	-78.3	1	96.5	103.6	100.0
f469n	MEB2	-78.1	1	17.8	18.8	18.3
f475w	MEB1	-78.1	1	954.4	1028.6	991.5
f475x	MEB1	-78.1	1	2557.3	2751.0	2654.1
f487n	MEB2	-77.9	1	37.4	39.9	38.6
f502n	MEB1	-52	2	45.7	48.8	47.3
f502n	MEB1	-78.2	3	54.5	58.2	56.3
f502n	MEB2	-53.9	2	45.3	48.4	46.8
f502n	MEB2	-78.1	4	53.2	56.8	55.0
f547m	MEB2	-78.3	1	1036.5	1118.2	1077.4
f555w	MEB1	-78.2	6	2743.9	2948.7	2846.0
f555w	MEB2	-78.1	3	2611.5	2807.1	2709.3
f555w	MEB2	-53.8	1	2389.8	2578.4	2484.1
f600lp	MEB2	-78.3	1	26501.6	27941.8	27221.7
f606w	MEB1	-77.9	1	8029.6	8635.5	8332.6
f621m	MEB2	-78.1	1	2569.3	2747.6	2658.5
f625w	MEB1	-51.1	3	5534.0	5942.4	5738.2
f625w	MEB1	-78.1	6	6398.6	6857.6	6628.1

filter	instrument side	CCD temp	num images	chip 1 e^-/s/pix	chip 2 e^-/s/pix	average e^-/s/pix
f625w	MEB2	-53.8	2	5361.3	5740.5	5550.9
f625w	MEB2	-78.2	3	6244.5	6702.2	6473.3
f631n	MEB2	-78.1	1	234.6	250.6	242.6
f645n	MEB1	-51.9	2	347.6	366.1	356.9
f645n	MEB1	-78.1	5	394.8	414.9	404.9
f645n	MEB2	-53.7	2	345.0	363.4	354.2
f645n	MEB2	-78.3	3	392.1	413.3	402.7
f656n	MEB1	-78.3	1	86.4	93.12	89.7
f657n	MEB1	-51.8	2	594.8	612.4	603.6
f657n	MEB1	-78.2	4	668.6	691.5	680.0
f657n	MEB2	-53.6	2	590.2	607.9	599.0
f657n	MEB2	-78.2	4	661.5	685.1	673.3
f658n	MEB1	-78.1		217.7	233.3	225.5
f658n	MEB2	-78.3	1	216.9	232.1	224.5
f665n	MEB2	-78.1	1	711.1	767.4	739.2
f673n	MEB2	-78.1	1	690.3	735.0	712.7
f680n	MEB2	-78.1	1	2384.4	2548.4	2466.4
f689m	MEB2	-77.9	1	4377.8	4694.0	4535.9
f763m	MEB2	-77.9	1	6228.5	6694.8	6461.7
f775w	MEB1	-77.9	1	11917.6	12888.3	12403.0
f814w	MEB1	-78.3	7	19237.0	20241.3	19739.2
f814w	MEB2	-54.3	1	18818.8	19782.7	19300.8
f814w	MEB2	-78.0	3	19155.2	20158.7	19657.0
f845m	MEB2	-78.3	1	7089.7	7520.9	7305.3
f850lp	MEB1	-78.3	1	10220.3	10582.5	10401.4
f953n	MEB1	-78.1	1	494.2	507.6	500.9
quad filters						
fq387n	MEB2	-78.1	2	--	--	1.9
fq422m	MEB2	-78.1	2	--	--	12.7
fq436n	MEB2	-78.1	2	--	--	8.9
fq492n	MEB2	-78.1	2	--	--	81.6
fq508n	MEB2	-77.9	1	--	--	114.5

filter	instrument side	CCD temp	num images	chip 1 e^-/s/pix	chip 2 e^-/s/pix	average e^-/s/pix
fq575n	MEB2	-77.9	1	--	--	40.5
fq619n	MEB2	-78.3	1	--	--	226.3
fq634n	MEB2	-78.3	1	--	--	274.4
fq672n	MEB2	-77.9	1	--	--	126.8
fq674n	MEB2	-77.9	1	--	--	82.9
fq727n	MEB2	-78.3	1	--	--	527.3
fq750n	MEB2	-78.3	1	--	--	547.3
fq889n	MEB2	-78.1	1	--	--	677.7
fq906n	MEB2	-78.1	1	--	--	641.8
fq924n	MEB2	-78.1	1	--	--	679.1
fq937n	MEB2	-78.1	1	--	--	619.2

Table 4. UVIS deuterium lamp countrates from TV2. Median level is for entire FOV except for quad filters, where median is that of the appropriate quadrant for the filter listed. Images were all taken at medium current.

filter	instrument side	CCD temp	date-obs	exptime (sec)	median level (e^-/s/pix)	ratio
f200lp	meb1	-78.1	2007-07-29	4.0	11070.4	1.00
f200lp	meb2	-78.1	2007-08-07	3.6	11082.5	1.00
f200lp	meb1	-78.5	2007-09-04	3.6	11010.9	0.99
f218w	meb2	-77.7	2007-06-24	45.0	835.3	1.00
f218w	meb2	-77.9	2007-06-29	46.0	878.6	1.05
f218w	meb2	-78.1	2007-07-04	46.0	863.0	1.03
f218w	meb1	-77.9	2007-07-12	46.0	913.3	1.09
f218w	meb1	-78.3	2007-07-17	46.0	911.6	1.09
f218w	meb2	-78.1	2007-07-23	45.0	895.7	1.07
f218w	meb1	-78.3	2007-07-23	45.0	899.1	1.08
f218w	meb1	-78.5	2007-07-25	46.0	933.0	1.12
f218w	meb1	-78.3	2007-07-29	44.5	865.1	1.04
f218w	meb1	-78.1	2007-08-02	46.0	859.4	1.03
f218w	meb2	-78.3	2007-08-10	46.0	839.2	1.00
f225w	meb1	-78.1	2007-07-29	17.4	1839.9	1.00

filter	instrument side	CCD temp	date-obs	exptime (sec)	median level (e^-/s/pix)	ratio
f225w	meb2	-78.3	2007-08-07	21.5	1883.6	1.02
f225w	meb1	-78.3	2007-09-04	21.5	1880.9	1.02
f275w	meb1	-77.9	2007-07-29	35.5	1072.2	1.00
f275w	meb2	-78.1	2007-08-07	38.0	1037.8	0.97
f275w	meb1	-78.3	2007-09-04	38.0	1033.5	0.96
f280n	meb1	-78.3	2007-07-29	745.0	43.8	1.00
f280n	meb2	-77.9	2007-08-07	941.0	43.0	0.98
f280n	meb1	-77.9	2007-09-04	941.0	43.0	0.98
f300x	meb1	-78.5	2007-07-29	18.4	2176.8	1.00
f300x	meb2	-78.3	2007-08-07	18.6	2158.2	0.99
f300x	meb1	-78.5	2007-09-04	18.6	2111.0	0.97
f336w	meb1	-78.3	2007-07-29	60.9	635.5	1.00
f336w	meb2	-78.1	2007-08-07	64.8	612.4	0.96
f336w	meb1	-78.3	2007-09-04	64.8	604.1	0.95
f343n	meb1	-78.5	2007-07-29	148.9	259.2	1.00
f373n	meb1	-77.9	2007-07-29	700.0	28.6	1.00
f390m	meb1	-78.1	2007-07-29	289.6	135.2	1.00
f390w	meb1	-77.9	2007-07-29	42.0	673.5	1.00
f390w	meb2	-78.1	2007-08-07	61.0	655.7	0.97
f390w	meb1	-78.1	2007-09-04	61.0	648.7	0.96
f395n	meb1	-78.3	2007-07-29	1000.0	56.7	1.00
quad filters						
fq232n	meb1	-78.1	2007-07-29	700.0	58.0	1.00
fq232n	meb1	-78.1	2007-07-29	700.0	55.9	0.96
fq232n	meb1	-78.1	2007-07-29	700.0	56.7	0.98
fq232n	meb1	-78.3	2007-07-29	700.0	54.9	0.95
fq243n	meb1	-78.1	2007-07-29	700.0	69.0	1.00
fq243n	meb1	-78.1	2007-07-29	700.0	67.0	0.97
fq243n	meb1	-78.1	2007-07-29	700.0	67.8	0.98
fq243n	meb1	-78.3	2007-07-29	700.0	65.8	0.95
fq378n	meb1	-78.1	2007-07-29	700.0	66.9	1.00

filter	instrument side	CCD temp	date-obs	exptime (sec)	median level (e^-/s/pix)	ratio
fq378n	meb1	-78.1	2007-07-29	700.0	65.4	0.98
fq378n	meb1	-78.1	2007-07-29	700.0	65.8	0.98
fq378n	meb1	-78.3	2007-07-29	700.0	64.4	0.96
fq387n	meb1	-78.3	2007-07-29	700.0	18.7	1.00
fq387n	meb1	-78.3	2007-07-29	700.0	18.7	1.00
fq387n	meb1	-78.5	2007-07-29	700.0	18.4	0.98
fq422m	meb1	-78.3	2007-07-29	700.0	43.6	1.00
fq422m	meb1	-78.3	2007-07-29	700.0	43.8	1.00
fq422m	meb1	-78.5	2007-07-29	700.0	43.2	0.99
fq436n	meb1	-78.3	2007-07-29	700.0	15.7	1.00
fq436n	meb1	-78.3	2007-07-29	700.0	15.7	1.00
fq436n	meb1	-78.5	2007-07-29	700.0	15.6	0.99
fq437n	meb1	-78.1	2007-07-29	700.0	12.7	1.00
fq437n	meb1	-78.1	2007-07-29	700.0	12.3	0.97
fq437n	meb1	-78.1	2007-07-29	700.0	12.5	0.98
fq437n	meb1	-78.3	2007-07-29	700.0	12.1	0.95
fq492n	meb1	-78.3	2007-07-29	700.0	28.2	1.00
fq492n	meb1	-78.3	2007-07-29	700.0	28.1	0.99
fq492n	meb1	-78.5	2007-07-29	700.0	28.1	0.99

Table 5. IR tungsten lamp calsystem countrates from TV2 as measured across the full FOV. Differences between full-frame and subarray countrates are discussed in text.

filter	lamp	side	obs date	obs time	sampseq (nsamp)	sqsize	median level (e^-/s/p)	ratio
f098m	tungsten-1	meb1	07-12-2007	22:04:30.67	step25 (15)	74	122.2	1.000
f098m	tungsten-1	meb1	07-17-2007	02:39:31.67	step25 (15)	74	120.9	0.990
f098m	tungsten-1	meb1	07-25-2007	16:26:36.67	step25 (15)	74	121.8	0.997
f098m	tungsten-1	meb1	07-30-2007	09:54:32.42	step100 (11)	1024	104.0	0.852
f098m	tungsten-1	meb1	08-02-2007	22:06:24.67	step25 (15)	74	121.6	0.995
f098m	tungsten-1	meb1	10-02-2007	08:59:19.68	step25 (15)	74	123.6	1.011
f098m	tungsten-1	meb2	06-29-2007	22:05:28.68	step25 (10)	74	133.7	1.000
f098m	tungsten-1	meb2	07-05-2007	00:13:26.67	step25 (15)	74	122.8	0.918
f098m	tungsten-1	meb2	08-09-2007	19:38:24.67	step25 (15)	74	122.5	0.916
f098m	tungsten-3	meb1	07-12-2007	22:16:01.68	step25 (15)	74	131.4	1.000
f098m	tungsten-3	meb1	07-17-2007	02:51:02.68	step25 (15)	74	130.8	0.996
f098m	tungsten-3	meb1	07-25-2007	16:38:07.68	step25 (15)	74	129.9	0.989
f098m	tungsten-3	meb1	08-02-2007	22:17:55.68	step25 (15)	74	130.6	0.994
f098m	tungsten-3	meb1	10-02-2007	09:11:48.67	step25 (15)	74	136.4	1.038
f098m	tungsten-3	meb2	06-29-2007	22:13:50.66	step25 (10)	74	141.3	1.000
f098m	tungsten-3	meb2	07-05-2007	00:24:57.68	step25 (15)	74	130.4	0.923
f098m	tungsten-3	meb2	08-09-2007	19:49:55.68	step25 (15)	74	132.7	0.939
f105w	tungsten-1	meb1	07-30-2007	10:01:42.41	step100(9)	1024	240.2	1.000
f110w	tungsten-1	meb1	07-30-2007	10:39:23.40	spars10(10)	1024	515.9	1.000
f125w	tungsten-1	meb1	07-30-2007	10:05:36.42	spars10 (14)	1024	382.5	1.000
f125w	tungsten-1	meb1	08-02-2007	02:22:35.40	spars25 (7)	1024	381.9	0.999
f125w	tungsten-1	meb1	08-02-2007	02:25:28.39	spars25 (7)	1024	385.2	1.007
f125w	tungsten-1	meb1	08-02-2007	02:28:21.42	spars25 (7)	1024	385.8	1.009
f125w	tungsten-1	meb1	08-02-2007	02:31:14.41	spars25 (7)	1024	385.2	1.007
f125w	tungsten-1	meb1	08-02-2007	02:43:45.42	spars25 (7)	1024	382.4	1.000
f125w	tungsten-1	meb1	08-02-2007	02:46:38.41	spars25 (7)	1024	385.1	1.007
f125w	tungsten-1	meb1	08-02-2007	02:49:31.40	spars25 (7)	1024	382.6	1.000
f125w	tungsten-1	meb1	08-02-2007	02:52:24.39	spars25 (7)	1024	382.0	0.999
f125w	tungsten-1	meb1	08-02-2007	03:04:55.40	spars25 (7)	1024	383.6	1.003
f125w	tungsten-1	meb1	08-02-2007	03:07:48.39	spars25 (7)	1024	383.4	1.002
f125w	tungsten-1	meb1	08-02-2007	03:10:41.42	spars25 (7)	1024	382.7	1.001

filter	lamp	side	obs date	obs time	sampseq (nsamp)	sqsize	median level (e^-/s/p)	ratio
f125w	tungsten-1	meb1	08-02-2007	03:13:34.41	spars25 (7)	1024	383.5	1.003
f125w	tungsten-1	meb1	08-02-2007	03:26:05.42	spars25 (7)	1024	381.2	0.997
f125w	tungsten-1	meb1	08-02-2007	03:28:58.41	spars25 (7)	1024	384.2	1.005
f125w	tungsten-1	meb1	08-02-2007	03:31:51.40	spars25 (7)	1024	383.6	1.003
f125w	tungsten-1	meb1	08-02-2007	03:34:44.39	spars25 (7)	1024	382.3	1.000
f125w	tungsten-1	meb1	08-02-2007	03:47:15.40	spars25 (7)	1024	382.2	0.999
f125w	tungsten-1	meb1	08-02-2007	03:50:08.39	spars25 (7)	1024	382.4	1.000
f125w	tungsten-1	meb1	08-02-2007	03:53:01.42	spars25 (7)	1024	381.4	0.997
f125w	tungsten-1	meb1	08-02-2007	03:55:54.41	spars25 (7)	1024	381.7	0.998
f125w	tungsten-1	meb1	08-02-2007	04:08:25.42	spars25 (7)	1024	383.2	1.002
f125w	tungsten-1	meb1	08-02-2007	04:11:18.41	spars25 (7)	1024	383.5	1.003
f125w	tungsten-1	meb1	08-02-2007	04:14:11.40	spars25 (7)	1024	382.4	1.000
f125w	tungsten-1	meb1	08-02-2007	04:17:04.39	spars25 (7)	1024	382.2	0.999
f125w	tungsten-1	meb1	08-02-2007	04:29:35.40	spars25 (7)	1024	383.9	1.004
f125w	tungsten-1	meb1	10-02-2007	09:24:54.40	spars25 (7)	1024	387.9	1.014
f125w	tungsten-1	meb2	08-09-2007	00:43:34.40	spars25 (7)	1024	362.9	1.000
f125w	tungsten-1	meb2	08-09-2007	00:46:27.42	spars25 (7)	1024	366.0	1.008
f125w	tungsten-1	meb2	08-09-2007	00:49:20.42	spars25 (7)	1024	363.5	1.002
f125w	tungsten-1	meb2	08-09-2007	00:52:13.41	spars25 (7)	1024	364.9	1.005
f125w	tungsten-1	meb2	08-09-2007	01:04:44.42	spars25 (7)	1024	364.5	1.004
f125w	tungsten-1	meb2	08-09-2007	01:07:37.41	spars25 (7)	1024	364.9	1.006
f125w	tungsten-1	meb2	08-09-2007	01:10:30.40	spars25 (7)	1024	364.3	1.004
f125w	tungsten-1	meb2	08-09-2007	01:13:23.42	spars25 (7)	1024	363.8	1.002
f125w	tungsten-1	meb2	08-09-2007	01:25:54.40	spars25 (7)	1024	362.8	1.000
f125w	tungsten-1	meb2	08-09-2007	01:28:47.42	spars25 (7)	1024	363.0	1.000
f125w	tungsten-1	meb2	08-09-2007	01:31:40.42	spars25 (7)	1024	364.1	1.003
f125w	tungsten-1	meb2	08-09-2007	01:34:33.41	spars25 (7)	1024	363.1	1.001
f125w	tungsten-1	meb2	08-09-2007	01:47:04.42	spars25 (7)	1024	363.6	1.002
f125w	tungsten-1	meb2	08-09-2007	01:49:57.41	spars25 (7)	1024	361.7	0.997
f125w	tungsten-1	meb2	08-09-2007	01:52:50.40	spars25 (7)	1024	362.5	0.999
f125w	tungsten-1	meb2	08-09-2007	01:55:43.42	spars25 (7)	1024	360.9	0.994
f125w	tungsten-1	meb2	08-09-2007	02:08:14.40	spars25 (7)	1024	361.5	0.996
f125w	tungsten-1	meb2	08-09-2007	02:11:07.42	spars25 (7)	1024	362.2	0.998

filter	lamp	side	obs date	obs time	sampseq (nsamp)	sqsize	median level (e^-/s/p)	ratio
f125w	tungsten-1	meb2	08-09-2007	02:14:00.42	spars25 (7)	1024	361.2	0.995
f125w	tungsten-1	meb2	08-09-2007	02:16:53.41	spars25 (7)	1024	361.7	0.997
f125w	tungsten-1	meb2	08-09-2007	02:29:24.42	spars25 (7)	1024	362.8	1.000
f125w	tungsten-1	meb2	08-09-2007	02:32:17.41	spars25 (7)	1024	362.0	0.997
f125w	tungsten-1	meb2	08-09-2007	02:35:10.40	spars25 (7)	1024	362.0	0.997
f125w	tungsten-1	meb2	08-09-2007	02:38:03.42	spars25 (7)	1024	360.5	0.993
f125w	tungsten-1	meb2	08-09-2007	02:50:34.40	spars25 (7)	1024	360.5	0.993
f126n	tungsten-1	meb1	07-30-2007	12:51:04.42	step400(16)	1024	18.4	1.000
f127m	tungsten-1	meb1	07-30-2007	10:19:53.42	step100(12)	1024	96.2	1.000
f128n	tungsten-1	meb1	07-30-2007	13:38:18.41	step400(15)	1024	21.2	1.000
f130n	tungsten-1	meb1	07-30-2007	14:18:47.40	step400(15)	1024	22.9	1.000
f132n	tungsten-1	meb1	07-30-2007	15:04:52.42	step400(15)	1024	22.3	1.000
f139m	tungsten-1	meb1	07-30-2007	10:28:43.40	step100(13)	1024	86.8	1.000
f140w	tungsten-1	meb1	07-30-2007	11:10:42.41	spars10(11)	1024	568.4	1.000
f153m	tungsten-1	meb1	07-30-2007	10:49:26.41	step100(12)	1024	103.8	1.000
f160w	tungsten-1	meb1	07-12-2007	22:02:38.42	step25 (8)	1024	420.3	1.000
f160w	tungsten-1	meb1	07-17-2007	02:37:39.42	step25 (8)	1024	431.1	1.026
f160w	tungsten-1	meb1	07-25-2007	16:24:44.42	step25 (8)	1024	442.8	1.054
f160w	tungsten-1	meb1	07-30-2007	10:58:29.42	spars10 (15)	1024	419.5	0.998
f160w	tungsten-1	meb1	08-02-2007	22:04:32.42	step25 (8)	1024	429.3	1.021
f160w	tungsten-1	meb1	10-02-2007	08:49:03.42	step25 (8)	1024	427.1	1.016
f160w	tungsten-1	meb2	06-26-2007	23:07:00.39	rapid (6)	1024	391.3	1.000
f160w	tungsten-1	meb2	06-29-2007	22:04:33.42	rapid (7)	1024	431.3	1.000
f160w	tungsten-1	meb2	07-05-2007	00:11:34.42	step25 (8)	1024	429.2	0.995
f160w	tungsten-1	meb2	08-09-2007	19:36:32.42	step25 (8)	1024	415.0	0.962
f160w	tungsten-3	meb1	07-12-2007	22:14:09.39	step25 (8)	1024	450.6	1.000
f160w	tungsten-3	meb1	07-17-2007	02:49:10.39	step25 (8)	1024	461.4	1.024
f160w	tungsten-3	meb1	07-25-2007	16:36:15.42	step25 (8)	1024	468.8	1.040
f160w	tungsten-3	meb1	08-02-2007	22:16:03.39	step25 (8)	1024	456.7	1.014
f160w	tungsten-3	meb1	10-02-2007	09:09:56.42	step25 (8)	1024	460.4	1.022
f160w	tungsten-3	meb2	06-26-2007	23:17:48.39	rapid (6)	1024	421.4	1.000
f160w	tungsten-3	meb2	06-29-2007	22:12:55.40	rapid (7)	1024	456.9	1.000
f160w	tungsten-3	meb2	07-05-2007	00:23:05.39	step25 (8)	1024	454.4	0.995

filter	lamp	side	obs date	obs time	sampseq (nsamp)	sqsize	median level (e^-/s/p)	ratio
f160w	tungsten-3	meb2	08-09-2007	19:48:03.39	step25 (8)	1024	444.2	0.972
f164n	tungsten-1	meb1	07-30-2007	15:45:26.41	step400(13)	1024	28.8	1.000
f167n	tungsten-1	meb1	07-12-2007	22:08:36.69	step25 (16)	74	42.0	1.000
f167n	tungsten-1	meb1	07-17-2007	02:43:37.69	step25 (16)	74	42.6	1.015
f167n	tungsten-1	meb1	07-25-2007	16:30:42.69	step25 (16)	74	43.7	1.040
f167n	tungsten-1	meb1	07-30-2007	16:12:36.42	step400 (12)	1024	30.4	0.723
f167n	tungsten-1	meb1	08-02-2007	22:10:30.69	step25 (16)	74	42.2	1.005
f167n	tungsten-1	meb1	10-02-2007	09:03:25.70	step25 (16)	74	41.3	0.982
f167n	tungsten-1	meb2	06-29-2007	22:07:44.68	step25 (15)	74	43.2	1.000
f167n	tungsten-1	meb2	07-05-2007	00:17:32.69	step25 (16)	74	42.2	0.977
f167n	tungsten-1	meb2	08-09-2007	19:42:30.69	step25 (16)	74	41.9	0.971
f167n	tungsten-3	meb1	07-12-2007	22:20:07.66	step25 (16)	74	43.8	1.000
f167n	tungsten-3	meb1	07-17-2007	02:55:08.66	step25 (16)	74	44.2	1.011
f167n	tungsten-3	meb1	07-25-2007	16:42:13.70	step25 (16)	74	45.1	1.031
f167n	tungsten-3	meb1	08-02-2007	22:22:01.66	step25 (16)	74	43.8	1.000
f167n	tungsten-3	meb1	10-02-2007	09:19:20.67	step25 (16)	74	43.3	0.990
f167n	tungsten-3	meb2	06-29-2007	22:16:06.66	step25 (15)	74	44.7	1.000
f167n	tungsten-3	meb2	07-05-2007	00:29:03.66	step25 (16)	74	43.9	0.983
f167n	tungsten-3	meb2	08-09-2007	19:54:01.70	step25 (16)	74	44.1	0.986

Appendix B. Calsystem Flatfields

Figure 9: UVIS calsystem tungsten flatfields, shown with inverted +/-20% greyscale stretch (except FQ387N, F410M, F658N, which are at +/-50%).

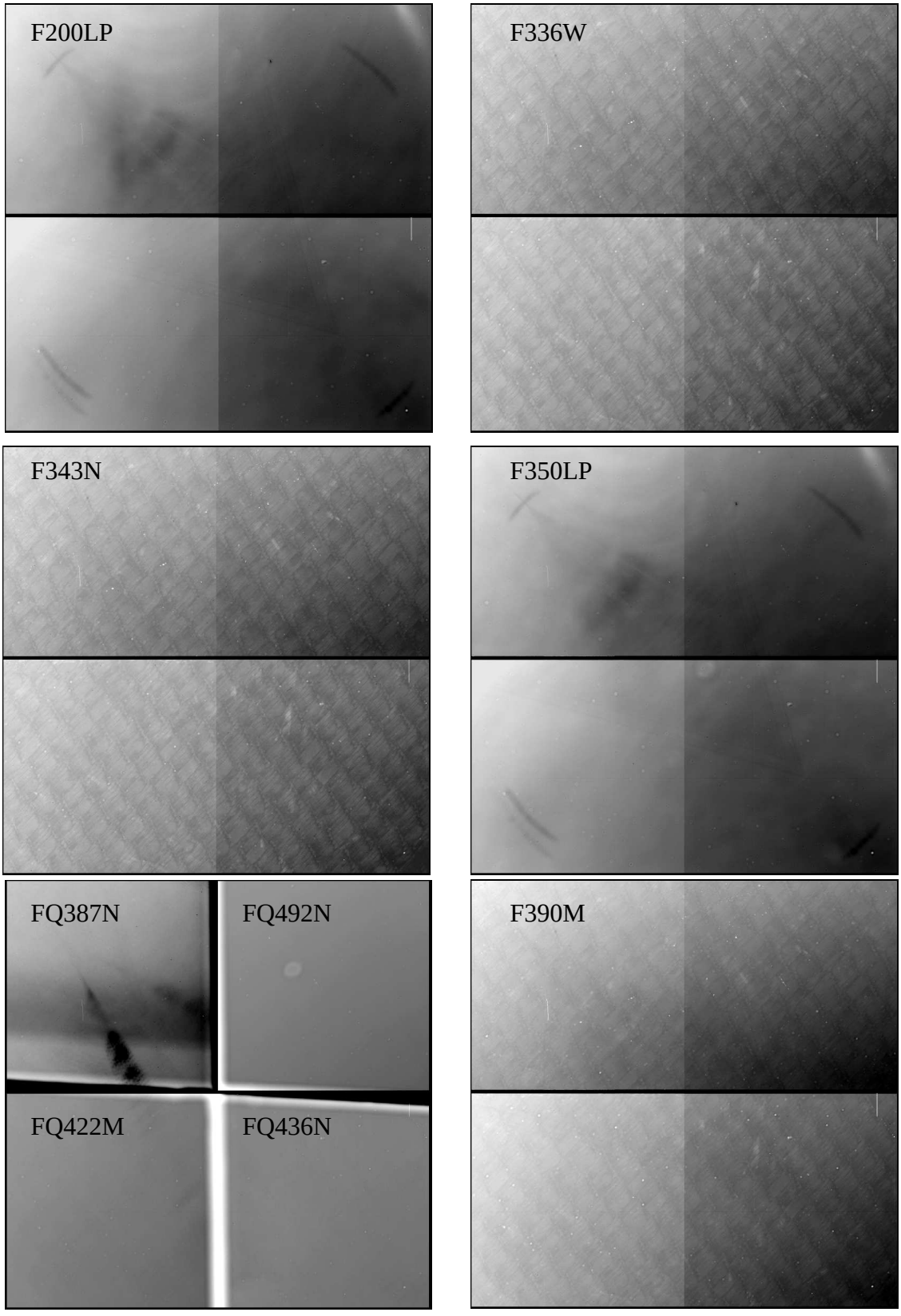

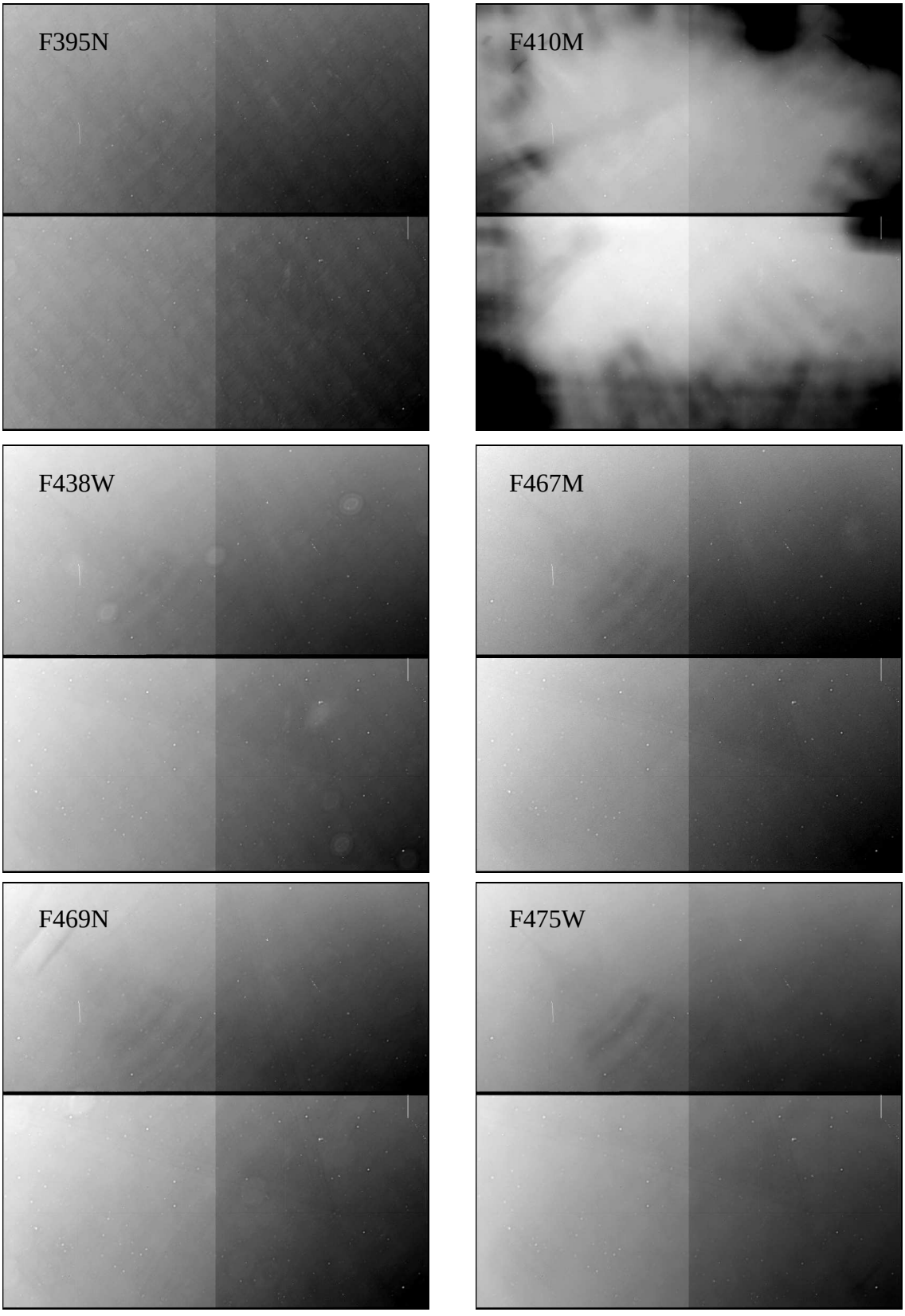
F395N
F410M
F438W
F467M
F469N
F475W

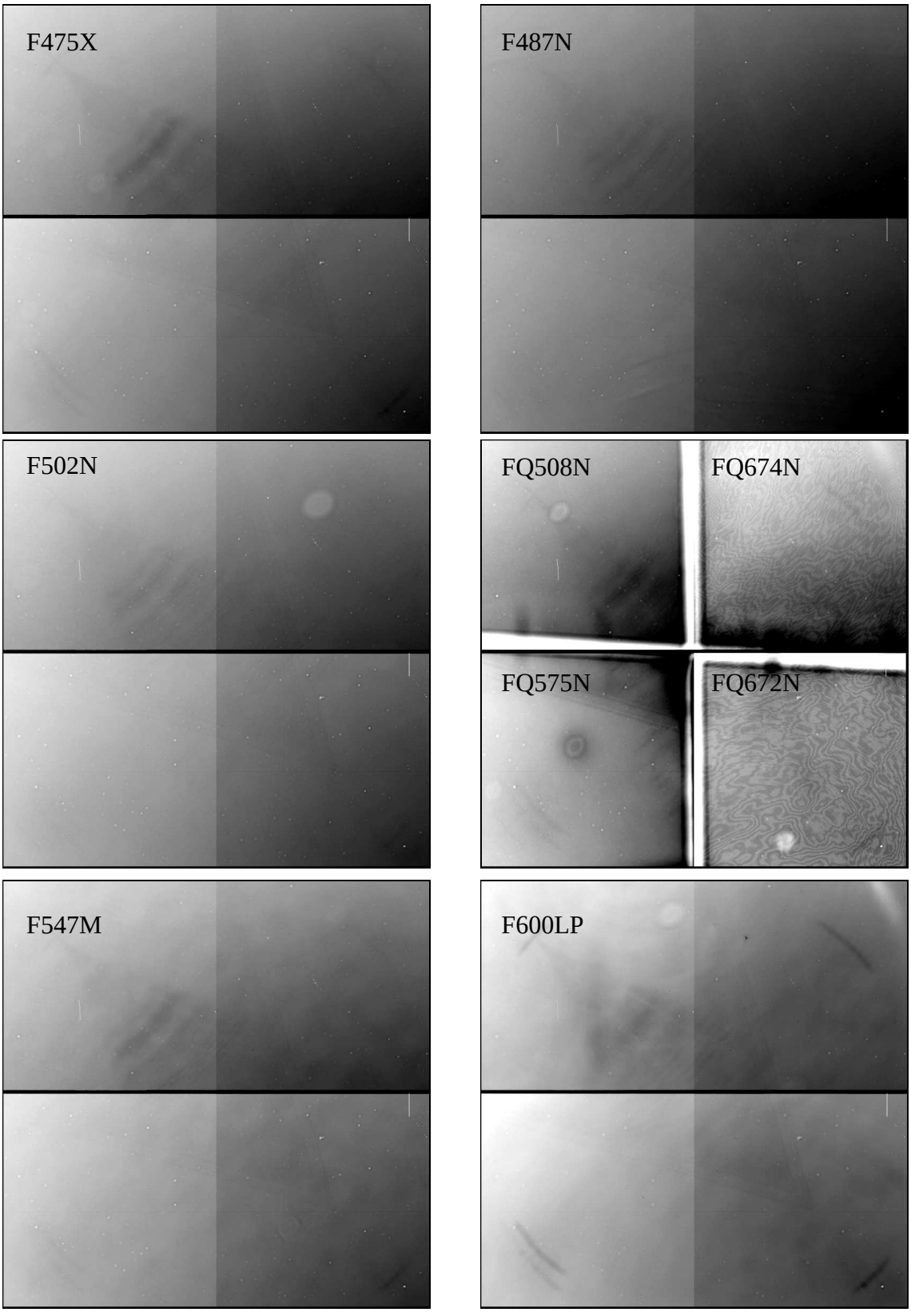
F475X
F487N
F502N
FQ508N
FQ674N
FQ575N
FQ672N
F547M
F600LP

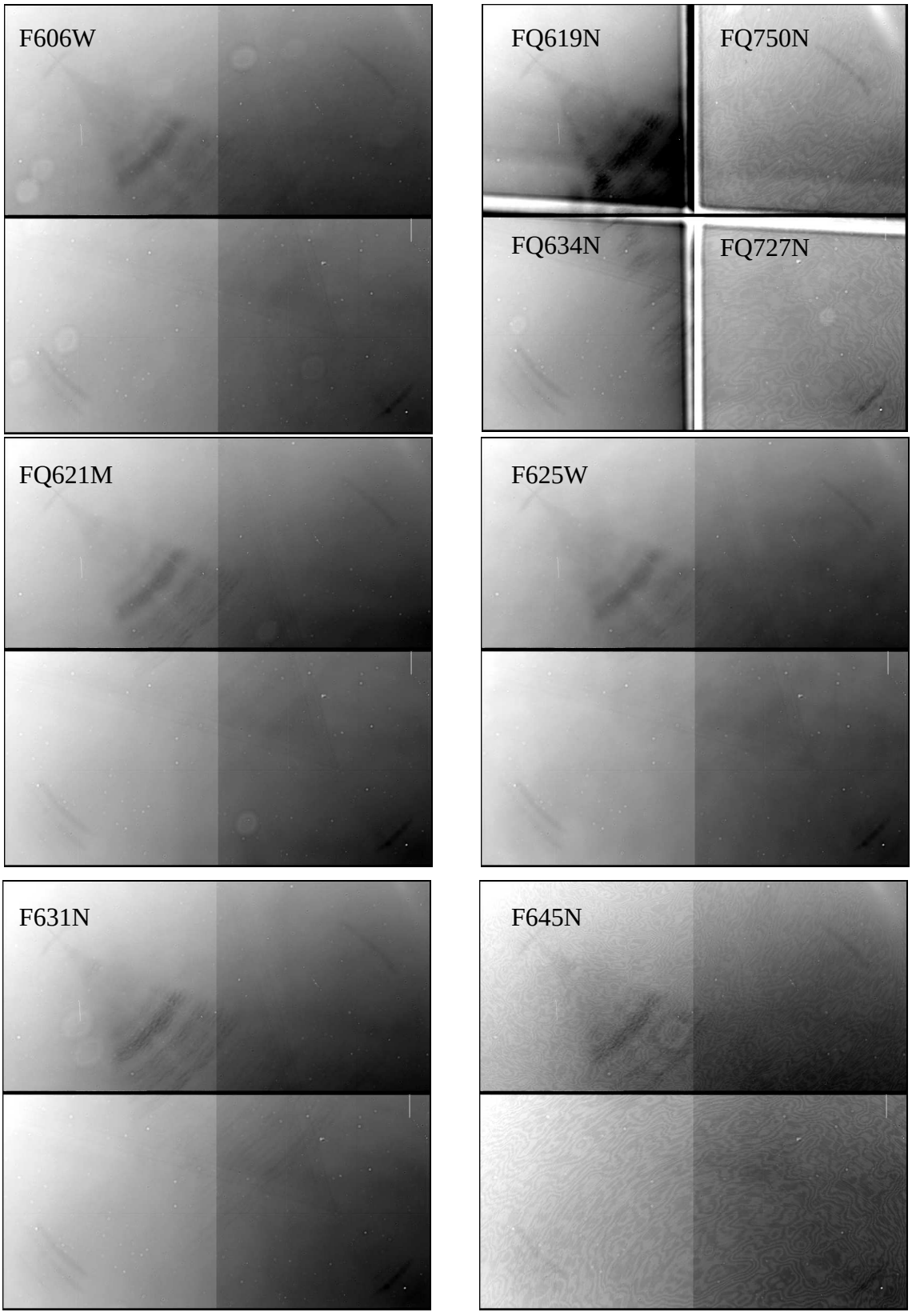
F606W
FQ619N
FQ750N
FQ634N
FQ727N
FQ621M
F625W
F631N
F645N

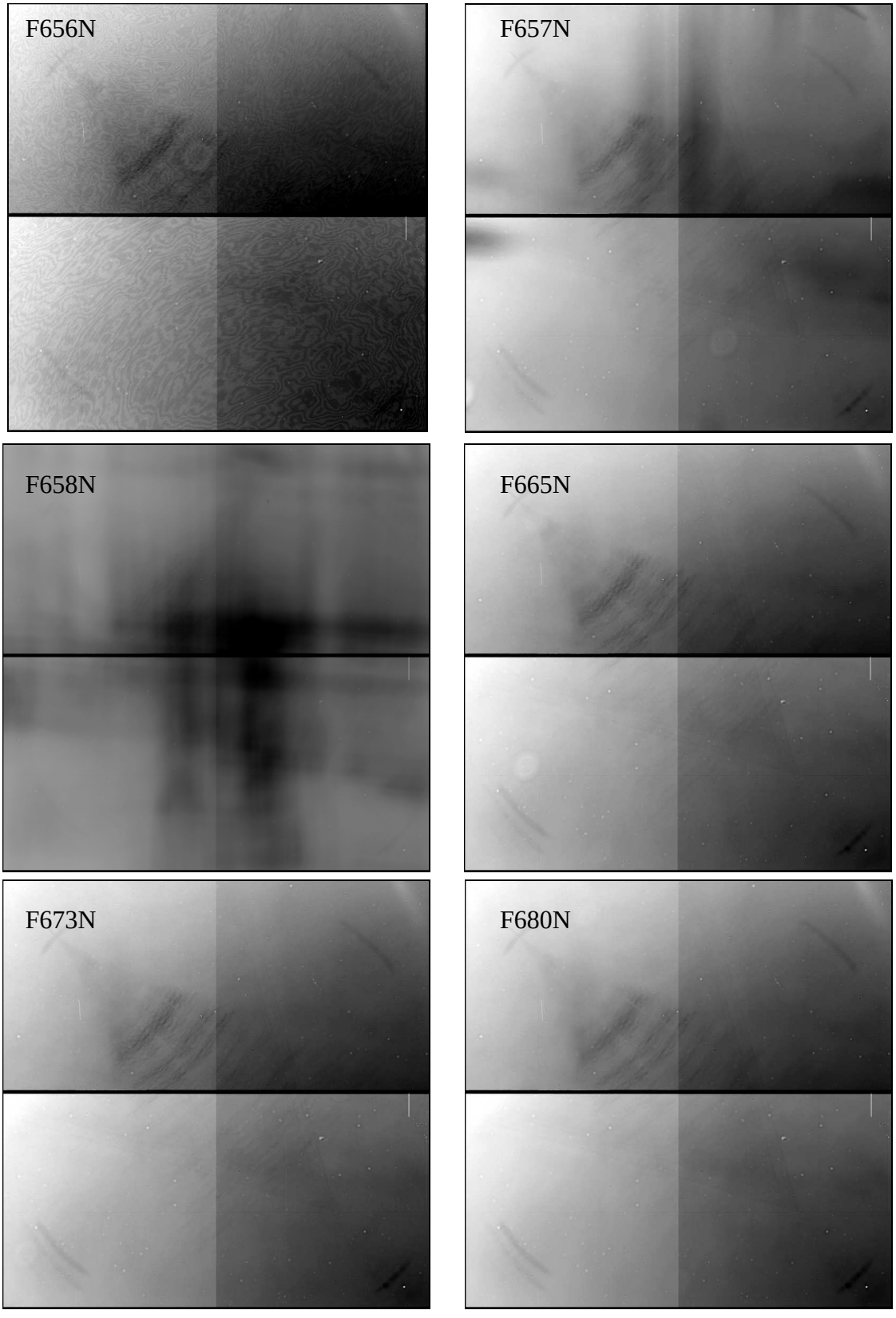
F656N
F657N
F658N
F665N
F673N
F680N

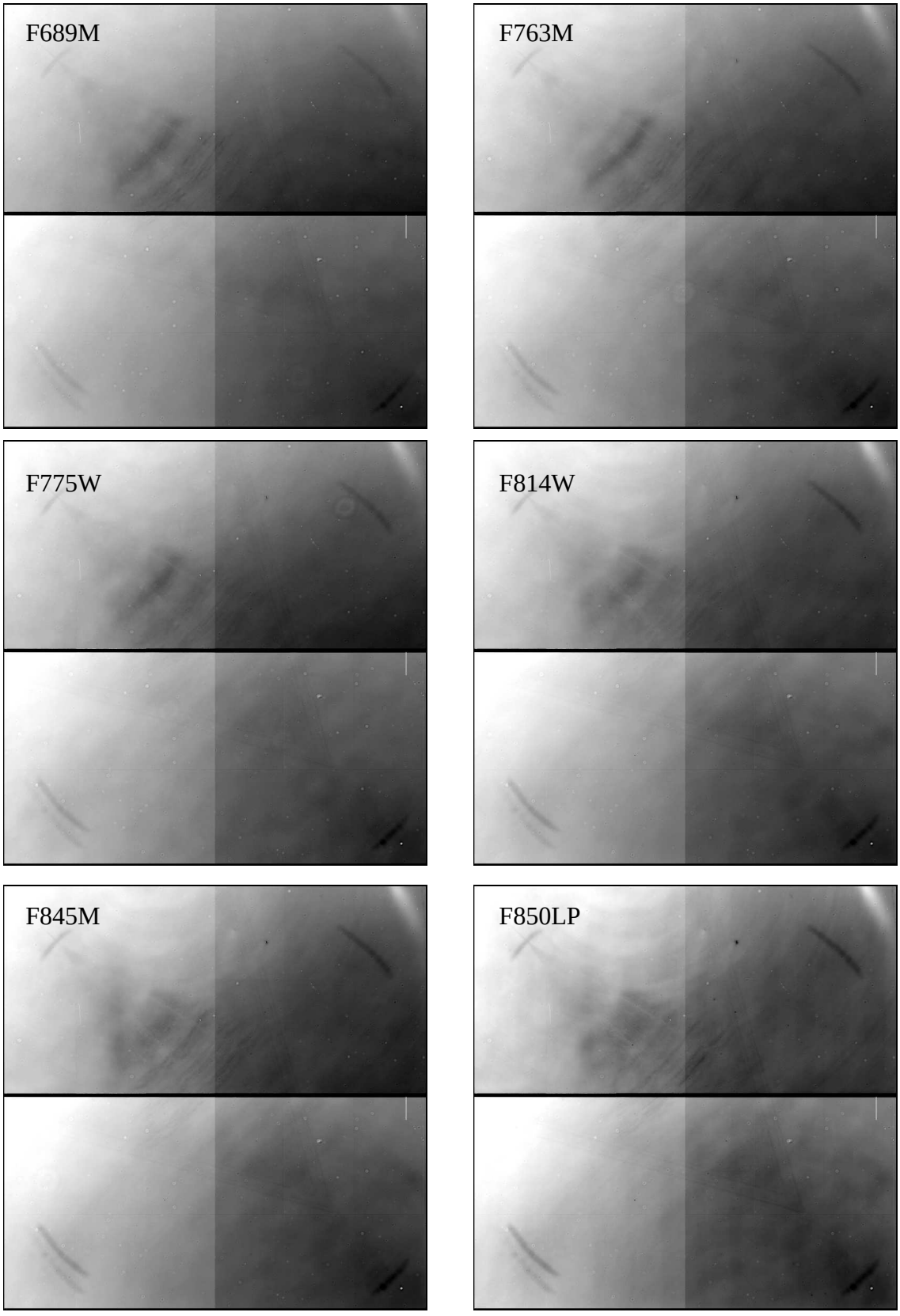
F689M
F763M
F775W
F814W
F845M
F850LP

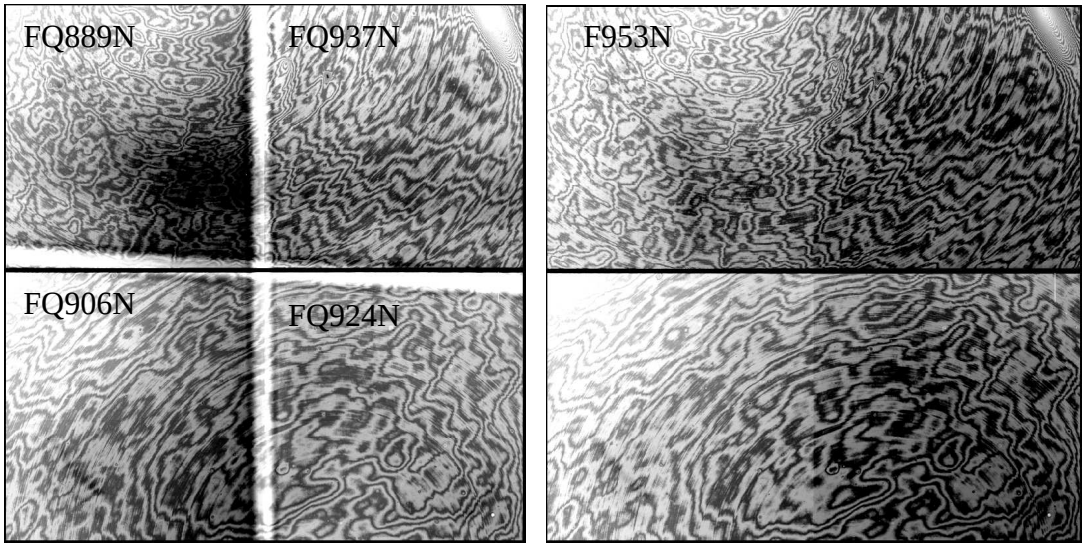
FQ889N
FQ937N
F953N
FQ906N
FQ924N

Figure 10: UVIS deuterium calsystem flatfields. Stretch is inverted +/-20% greyscale, +/-, (quad filters at +/-50%). F218W and F336W images are shown in text of report.

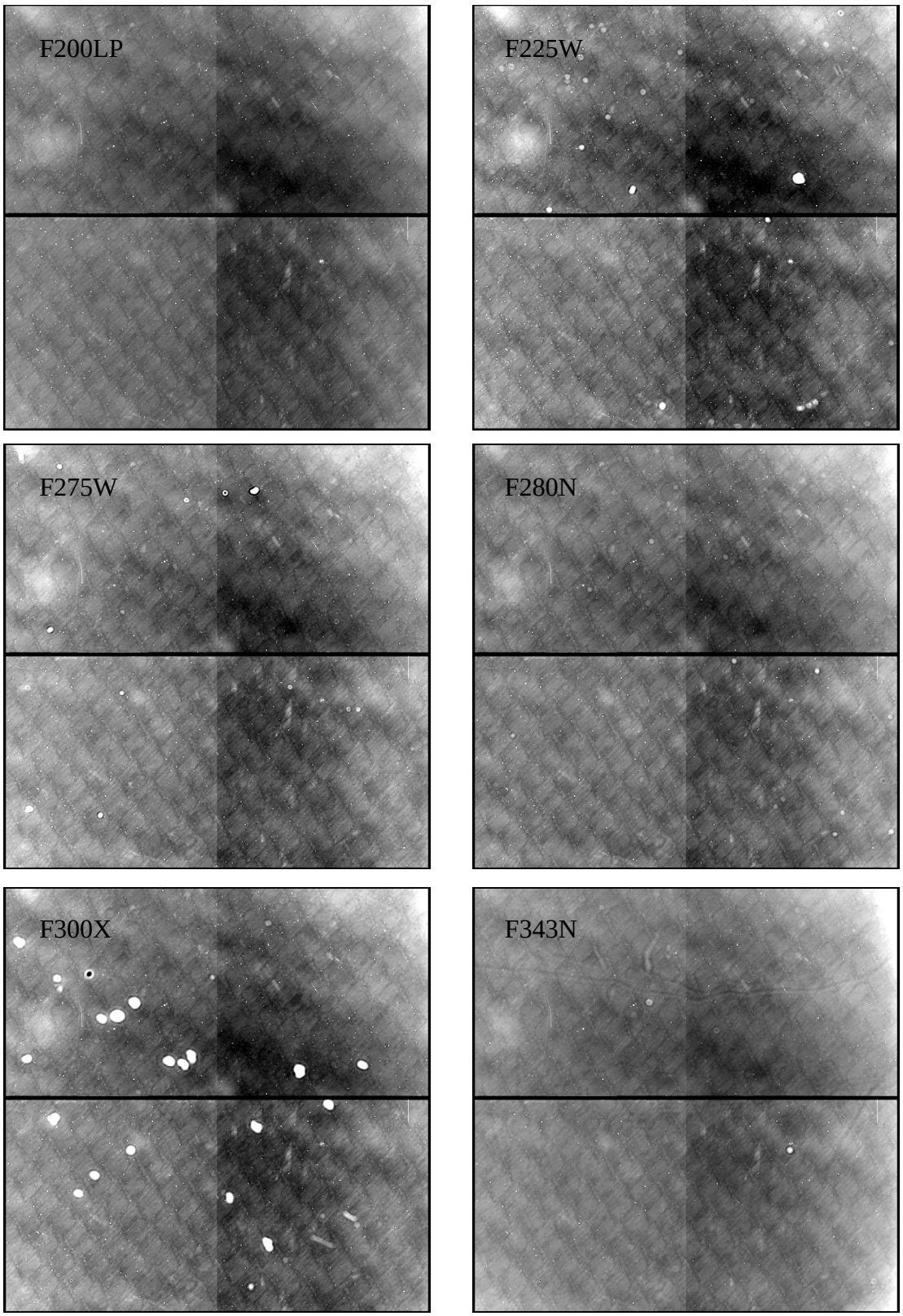

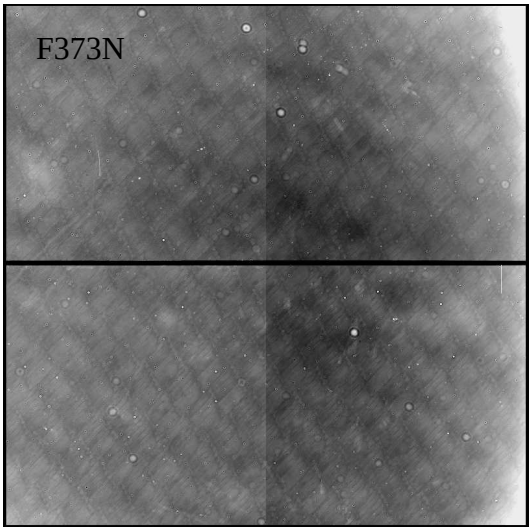
F373N

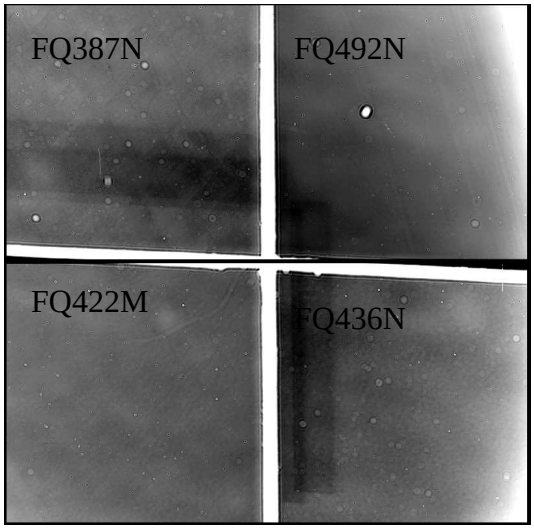
FQ387N
FQ492N
FQ422M
FQ436N

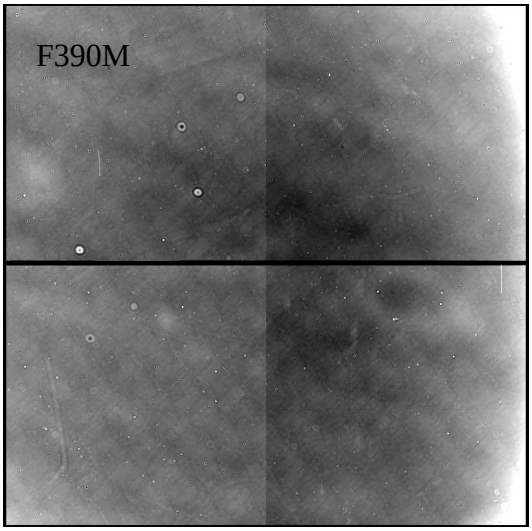
F390M

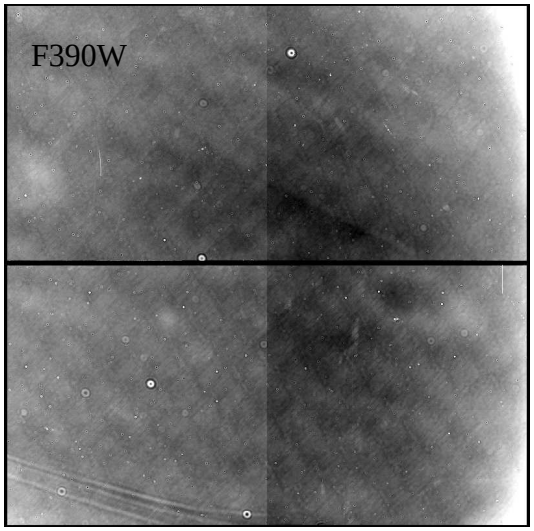
F390W

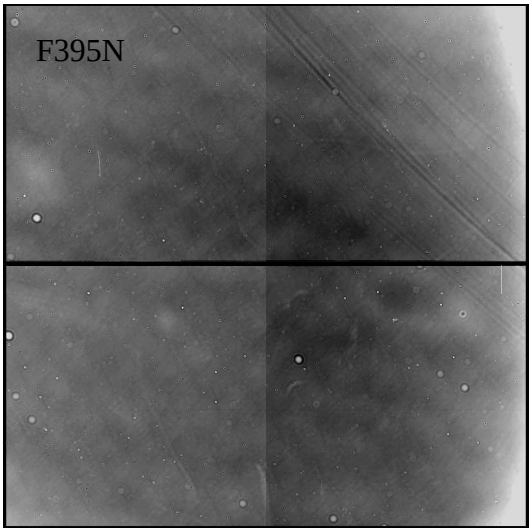
F395N

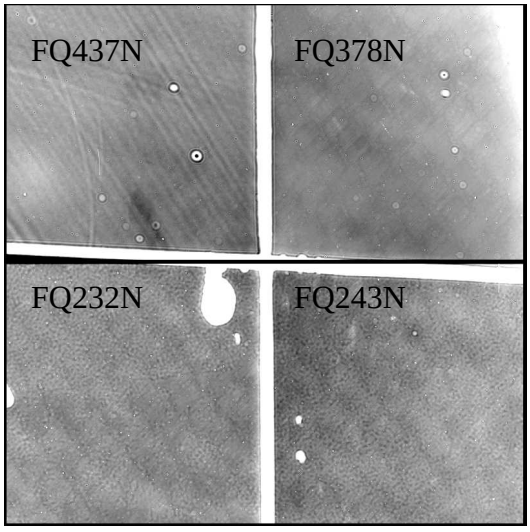
FQ437N
FQ378N
FQ232N
FQ243N

Figure 11: IR calsystem tungsten flatfields, shown with inverted +/-20% greyscale stretch.

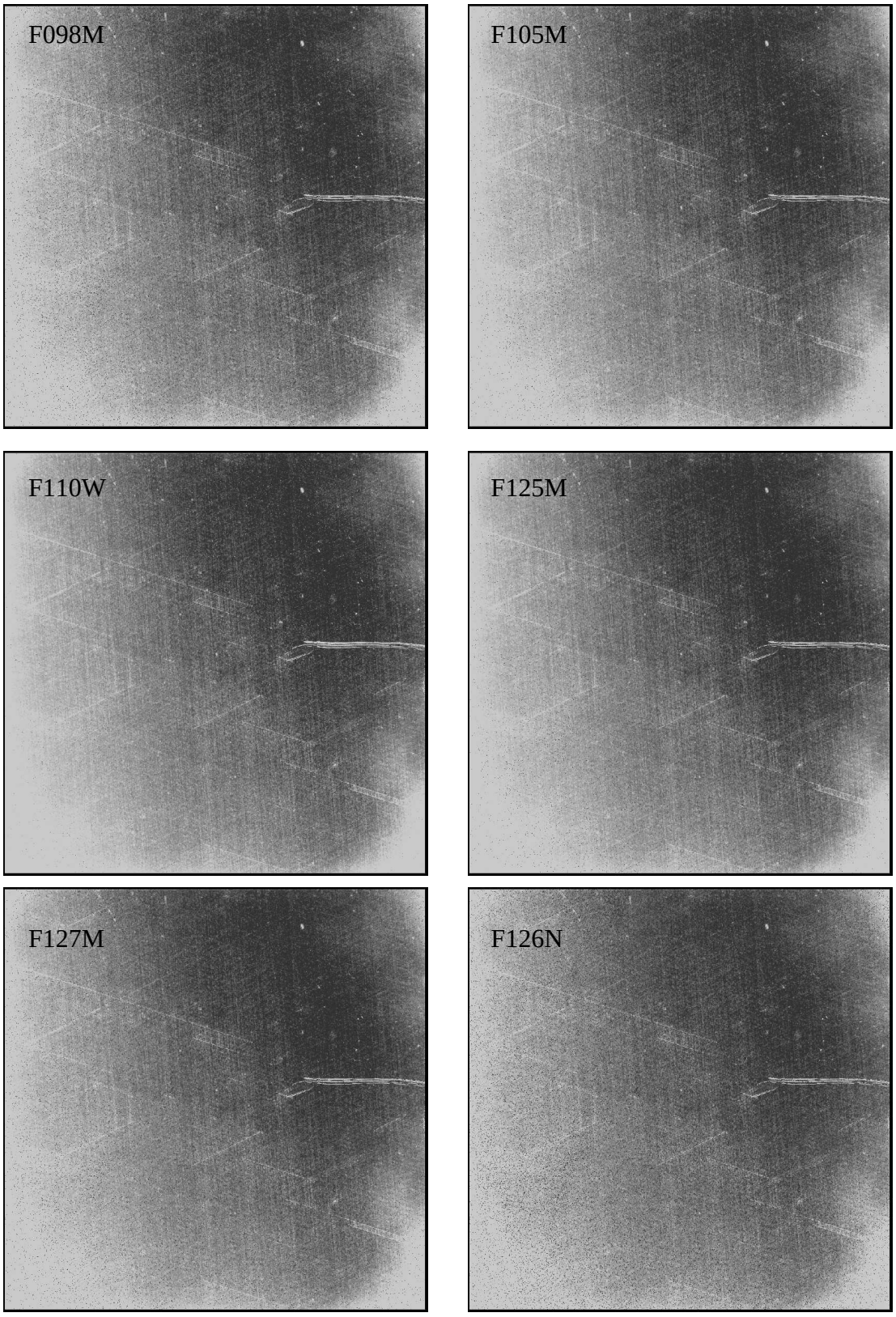

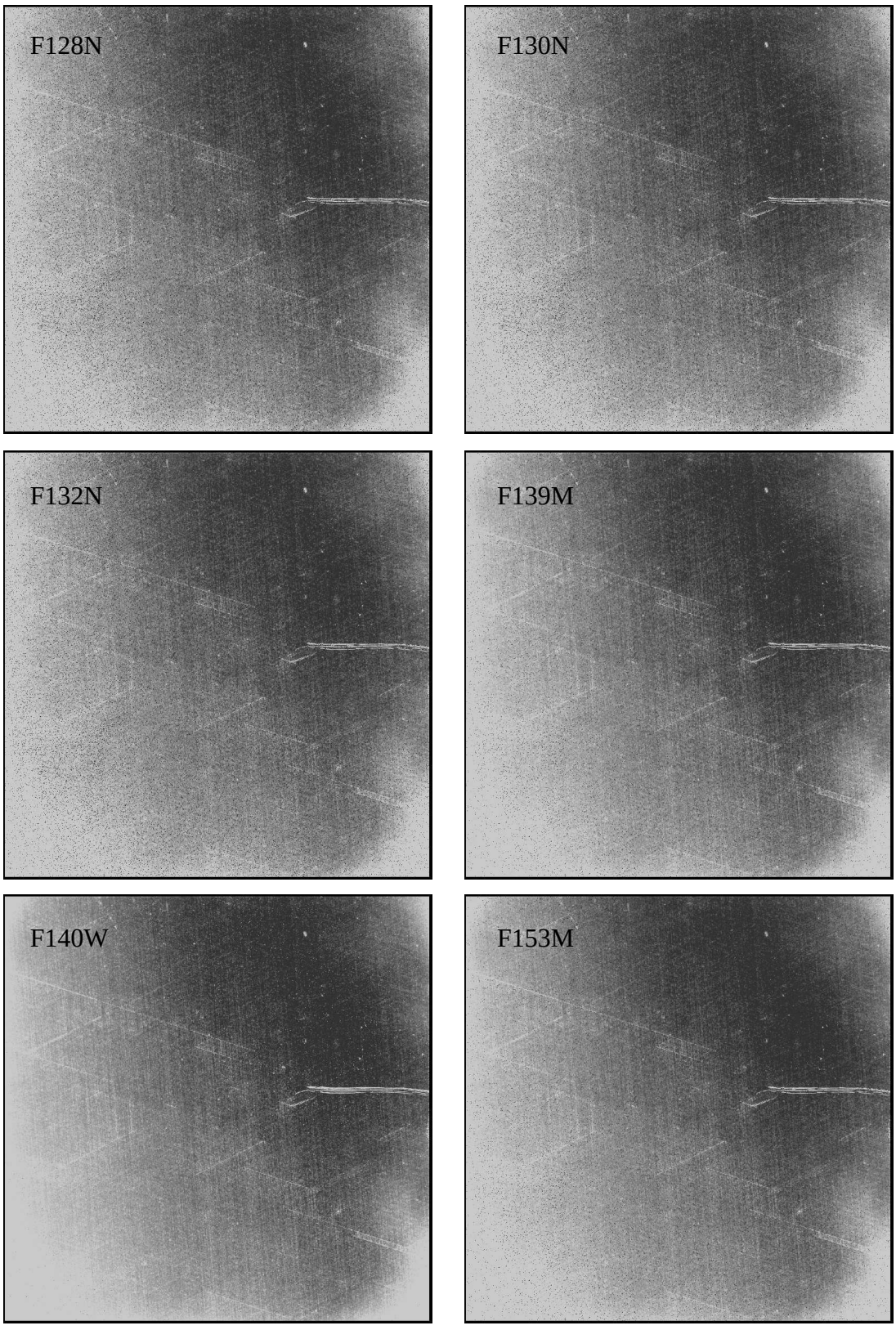
F128N
F130N
F132N
F139M
F140W
F153M

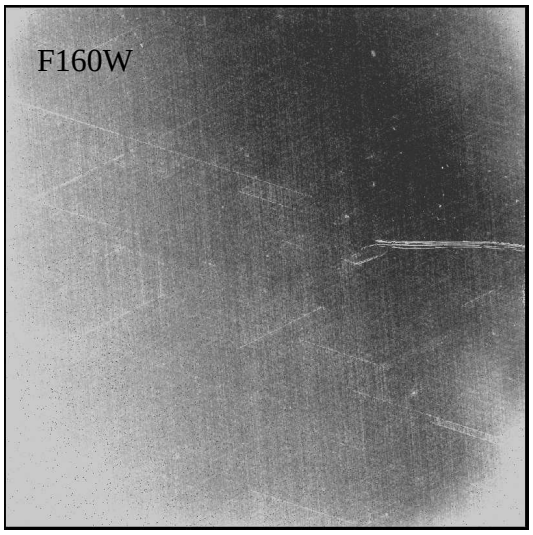
F160W

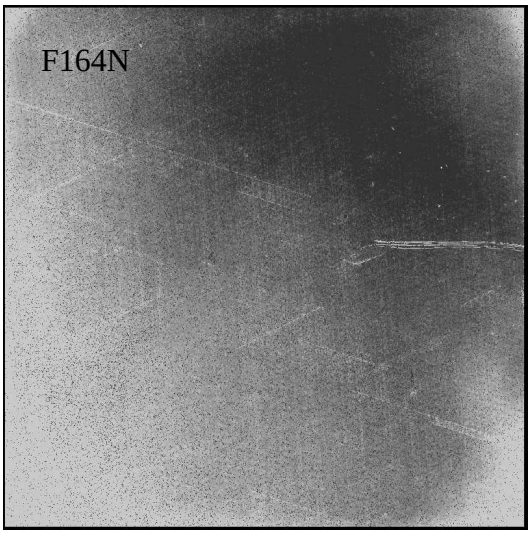
F164N


F167N